

School of Engineering and Digital Sciences
Nazarbayev University
Astana, Kazakhstan



NAZARBAYEV UNIVERSITY

Capstone Project II

Report 4

Design of Plant for Industrial Production of Methyl tert-butyl Ether in Kazakhstan

Supervisor: Aishuak Konarov

Course instructor: Dhawal Shah

Group members: Tomiris Zhumagaliyeva

Aidarkhan Akhmet

Aziza Kireyeva

Adina Kapsamatova

Aibar Alpysbayev

Yuliya Tyan

Date: 20.04.2024

Work distribution table

Chapter	Subsection	Tomiris	Aidarkhan	Aziza	Adina	Aibar	Yuliya
1	Process Introduction						
1.1	General Properties of Reactants and Products		1 st				
1.2	Uses and Applications of the Product		1 st				
1.3	Product Specification and Quality Requirements			1 st			
1.4	Production Rate Selection			1 st			
2	Process Summary						
2.1	Process Description and PFD			1 st	2 nd		
2.2	Material Balance			2 nd		1 st	
3	Major Equipment Design						
3.1	Reactor R-101 Design	1 st					
3.2	Compressor C-101 Design					1 st	
3.3	Heat Exchanger Design						
3.3.1	Heat Exchanger E-101 Design			1 st			
3.3.2	Heat Exchanger E-102 Design		1 st				

3.4	Distillation Column Design						
3.4.1	Distillation Column T-101 Design						1 st
3.4.2	Distillation Column T-103 Design				1 st		
4	Minor Equipment Design						
4.1	Distillation Column T-102 design	1 st					
4.2	Heaters and Coolers Design					1 st	
4.3	Pumps and Valves Design					1 st	
4.4	Storage Tanks Design						
4.4.1	MTBE Storage Tank Design	1 st				2 nd	
4.4.2	Methanol Storage Tank Design	1 st				2 nd	
5.	Plant Location and Layout						
5.1	Plant Location						1 st
5.1.1	Raw materials						1 st
5.1.2	Geographical Factors and Infrastructure						1 st
5.1.3	Governmental Policies &						1 st

	Economical Considerations						
5.2	Plant Layout				1 st		
5.2.1	Main Process and Storage Facilities				1 st		
5.2.2	Emergency Facilities				1 st		
5.2.3	Laboratory and Utilities				1 st		
5.2.4	Administrative and Personnel Areas				1 st		
6.	Environment and Waste Streams						
6.1	Butenes Stream Treatment					1 st	
6.2	Wastewater Stream Treatment					1 st	
7.	Total Investment and Profitability						
7.1	Cost of Equipment				1 st		
7.2	Capital Investment Estimation				1 st		
7.3	Operation Labor Estimation	1 st					
7.4	Fixed Costs of Production	1 st					
7.5	Variable Costs of Production	1 st			2 nd		
7.6	Cash Flow and Profitability	1 st			1 st		

	Estimation						
8.	Conclusions and Future Work						
						1 st	

Table of Contents

List of Figures	6
Chapter 1. Process introduction	9
1.1 General Properties of Reactants and Products	9
1.2. Uses and Applications of the Product.	9
1.3 Product Specification and Quality Requirements	10
1.4. Production Rate Selection	10
Chapter 2. Process Summary	11
2.1. Process Description and PFD	11
2.2. Material Balance	14
Chapter 3. Major Equipment Design	16
3.1 Reactor R-101 Design	16
3.2 Compressor C-101 Design	19
3.3 Heat Exchanger Design	24
3.3.1 Heat Exchanger E-101 Design	24
3.3.2 Heat Exchanger E-102 Design	27
3.4 Distillation Column Design	30
3.4.1 Distillation Column T-101 Design	32
3.4.2 Distillation Column T-103 Design	36
Chapter 4. Minor Equipment Design	40
4.1 Distillation Column T-102 design	40
4.2 Heaters and Coolers Design	41
4.3 Pumps and Valves Design	41
4.4 Storage Tanks Design	42

4.4.1 MTBE Storage Tank Design	42
4.4.2 Methanol Storage Tank Design	42
Chapter 5. Plant Location and Layout	43
5.1 Plant Location	43
5.1.1 Raw materials	43
5.1.2 Geographical Factors and Infrastructure	44
5.1.3 Governmental Policies & Economical Considerations	44
5.2 Plant Layout	44
5.2.1 Main Process and Storage Facilities	45
5.2.2 Emergency Facilities	45
5.2.3 Laboratory and Utilities	46
5.2.4 Administrative and Personnel Areas	46
Chapter 6. Environment and Waste Streams	46
6.1 Butenes Stream Treatment	46
6.2 Wastewater Stream Treatment	47
Chapter 7. Total Investment and Profitability	47
7.1 Cost of Equipment	47
7.2 Capital Investment Estimation	49
7.3 Operation Labor Estimation	50
7.4 Fixed Costs of Production	51
7.5 Variable Costs of Production	52
7.6 Cash Flow and Profitability Estimation	52
Chapter 8. Conclusions and Future Work	54
Reference List	55

List of Tables

Table 1.1. Main properties of MTBE [1].	9
Table 2.1. Temperature and pressure values for streams 1-11.	14
Table 2.2. Temperature and pressure values for streams 12-21.	14
Table 2.3. Mass balance for MTBE reactor R-101 with recycle.	14
Table 2.4. Total mass balance for T-101 column.	15
Table 2.5. Total mass balance for T-102 column.	15

Table 2.6. Total mass balance for T-103 column.	15
Table 2.7. Composition of the product by mass.	16
Table 3.1. Reactor R-101 specification sheet.	18
Table 3.2. Feed properties of the C-101 compressor.	20
Table 3.3. Outlet properties of the C-101 compressor.	21
Table 3.4. Compressor specifications.	21
Table 3.5. Comparison of hand calculated values and Aspen Plus V14 results.	25
Table 3.6. Specification sheet for E-101.	25
Table 3.8. Specification sheet for E-102.	28
Table 3.9. Hand calculated variables.	32
Table 3.10. Distillation Column T-101 specifications.	34
Table 3.11. Hand-calculated variables.	36
Table 3.12. Distillation Column T-103 specifications.	38
Table 4.1. Distillation Column T-102 specifications.	40
Table 4.2. Distillation Column T-102 specifications.	41
Table 4.3. Cooler specifications.	41
Table 4.4. Pump specifications.	41
Table 4.5. Valve specifications.	42
Table 4.6. MTBE storage tank specifications.	42
Table 4.7. Methanol storage tank specifications.	42
Table 6.1. Composition of stream 18.	46
Table 6.2. Composition of stream 20.	47
Table 7.1. Equipment and installation costs.	48
Table 7.2. Installation factors for equipment.	49
Table 7.3. Capital investment estimation.	50
Table 7.4. The equipment included in the N_{np} calculations.	50
Table 7.5. Fixed operation cost estimation.	51
Table 7.6. Variable cost of production.	52
Table 7.7. Economic parameters for profitability estimation.	53

List of Figures

Figure 1.1. MTBE's Molecular structure.	9
Figure 1.2. Extrapolated MTBE demand in CIS region, 2012-2021.	11
Figure 2.1 Process flow diagram.	12
Figure 3.1. MTBE synthesis reaction.	16
Figure 3.2. Simulation results and literature data for conversion of IB as a function of space time for 333 K [12].	17
Figure 3.3. Approximate ranges of compressor types used in petrochemical industries [16].	20

Figure 3.4. Impeller geometry. Subscripts: 1 blade leading edge midpoint, 2 blade trailing edge, E eye, H hub, B blade, b width [18].	23
Figure 3.5. 3D-impeller, shrouded with twisted backward-curved blades, b straight-line blade elements for 5-axis NC flank milling [18].	23
Figure 3.6. Single-shaft compressor with 4 impellers [18].	24
Figures 3.7a, 3.7b. Sensitivity analysis: Number of stages vs. Mass fraction of MTBE in the bottom.	33
Figures 3.8a, 3.8b. Sensitivity analysis: Feed stage vs Mass fraction of MTBE in the bottom.	33
Figure 3.9a, 3.9b. Sensitivity analysis: Reflux Ratio vs Mass fraction of MTBE in the bottom.	34
Figure 3.10a, 3.10b. Sensitivity analysis: Condenser pressure (bar) vs Mass fraction of MTBE in the bottom.	34
Figure 3.11. Sensitivity analysis: Number of stages vs. Mole fraction of MeOH in the distillate.	37
Figure 3.12. Sensitivity analysis: Feed stage vs. Mole fraction of MeOH in the distillate.	37
Figure 3.13. Sensitivity analysis: Distillate rate vs. Mole fraction of MeOH in the distillate.	38
Figure 5.1. Plant location.	43
Figure 5.2. Plant layout.	45
Figure 7.1. The Net Present Value for the first 20 years of operation.	53

List of Abbreviations

Abbreviation	Definition
APEA	Aspen Process Economic Analyzer
ASTM	American Society for Testing and Materials
CAS	Chemical Abstracts Service
CEPCI	Chemical Engineering Plant Cost Index
CIS	Commonwealth of Independent States
EBIT	Earnings Before Interest and Taxes
FUG	Fenske-Underwood-Gilliland
GDP	Gross Domestic Product
IB	Isobutylene
ID	Internal Diameter
IRR	Internal Rate of Return

ISBL	Inside Battery Limit
ISM	IS Med Specialties
IUPAC	International Union of Pure and Applied Chemistry
IZ	Industrial Zone
LHHW	Langmuir-Hinshelwood-Hougen-Watson
LMTD	Log Mean Temperature Difference
LOEC	Lowest Observed Effect Concentration
LPG	Liquified Petroleum Gas
MeOH	Methanol
MTBE	Methyl-Tert-Butyl-Ether
NOEC	No Observed Effect Concentration
NPV	Net Present Value
OD	Outer Diameter
OSBL	Outside Battery Limits
PFD	Process Flow Diagram
ROI	Return on Investment
RPM	Revolutions Per Minute
TEMA	Tubular Exchanger Manufacturers Association
UNIFAC	UNIQUAC Functional-group Activity Coefficients
WHSV	Weight Hourly Space Velocity
WWTP	Wastewater treatment plant

Chapter 1. Process introduction

1.1 General Properties of Reactants and Products

Methyl tert-butyl ether (MTBE), also known as 2-methoxy-2-methylpropane in IUPAC, and 1634-04-4 in CAS, is an ether which has a methyl group and a tert-butyl group and oxygen in between them. Its molecular structure is seen in Figure 1.1.

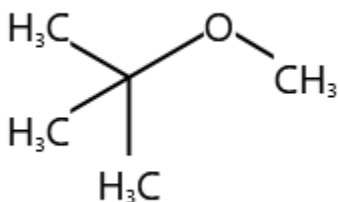


Figure 1.1. MTBE's Molecular structure.

Commercial MTBE is colorless, volatile liquid with gasoline-like odor. Its main identifiers are listed in Table 1.1. The more specific information on the properties of the raw materials and product are given in Appendices A, B, and C.

Table 1.1. Main properties of MTBE [1].

CAS name	Methyl tert-butyl ether
IUPAC Name	MTBE
CAS registry number	1634-04-4
Chemical formula	$(\text{CH}_3)_3\text{COCH}_3$
Molecular weight	88.15

1.2. Uses and Applications of the Product.

Methyl tertiary-butyl ether (MTBE) is a chemical compound predominantly used as a gasoline additive to improve combustion efficiency and reduce emissions of pollutants like carbon monoxide and unburned hydrocarbons. Its widespread use in reformulated gasoline during the 1990s significantly contributed to air quality improvements. However, MTBE's high water solubility and persistence in the environment have led to contamination concerns, particularly in groundwater, resulting from leaks in underground storage tanks. Despite these issues, MTBE remains useful in various other applications. For example, it is employed in extraction processes due to its efficacy as a solvent in separating complex mixtures, as detailed in studies on chemical extraction methods [2].

MTBE is primarily used in order to increase the octane number of the fuel by increasing thermal efficiency of an engine because of a more complete combustion. Because of more complete combustion the content of CO₂ is increased in the fumes thus minimizing harmful pollutants like CO. MTBE increases the efficiency of an engine at every level RPM thus it makes the work of an engine more balanced throughout time and it is helpful by increasing the fuel efficiency at low RPMs. [3]

MTBE is known to be a most efficient fuel additive in terms of increasing octane number compared to other additives like isooctene [4] and ethanol [5]. Increasing the octane number is important in preventing detonation which occurs when combustion of air/fuel mixture does not occur because of ignited spark, and it does not match with the four-stroke cycle. Detonation deteriorates engine's components and shortens its functional lifetime [5].

1.3 Product Specification and Quality Requirements

The standard specification for MTBE used in automotive spark-ignition engines, such as ASTM, mandates that the MTBE content must be at least 95% by mass [6]. Since the MTBE plant is going to be based in Kazakhstan, it is important to consider the standards set by the local government. According to "ST RK 2533-2021", a product of Grade B should include at least 96% of MTBE by mass, with a maximum allowed content of alcohols (methanol, tert-butyl alcohol) and hydrocarbons (C₄, C₈) set to 2.5% and 1.5% by mass, respectively. Density of the commercial product at 20°C should be 740 kg/m³ minimum [7].

1.4. Production Rate Selection

There is no explicit data about consumption and production rates in CIS region, therefore it was decided to extrapolate from known information about a particular region. Since data for the Chinese market was available, it constructed a base for forecasting demand and apparent production of MTBE for CIS and Kazakhstan. The estimation of MTBE demand in the CIS region was derived using a scaling approach based on nominal GDP, with China serving as the reference point. The calculation method involved first gathering data on MTBE demand in China and applying a scaling factor to estimate corresponding demand for the CIS. The scaling factor was calculated by comparing the nominal GDP of the CIS region to that of China, rather than focusing on per capita GDP. This allowed for a more accurate reflection of the economic activity and overall industrial output differences between the two regions. The detailed data used in calculations is given in Appendix D.

$$\text{Scaling factor} = \frac{\text{GDP of CIS}}{\text{GDP of China}}$$

This factor was then multiplied by the demand for MTBE in China to estimate the demand for the CIS:

$$MTBE \text{ Demand in CIS} = MTBE \text{ Demand in China} \times \text{Scaling factor}$$

For each year from 2018 to 2021, this method was applied and the following MTBE demand estimates (Fig. 1.2) for the CIS were obtained:

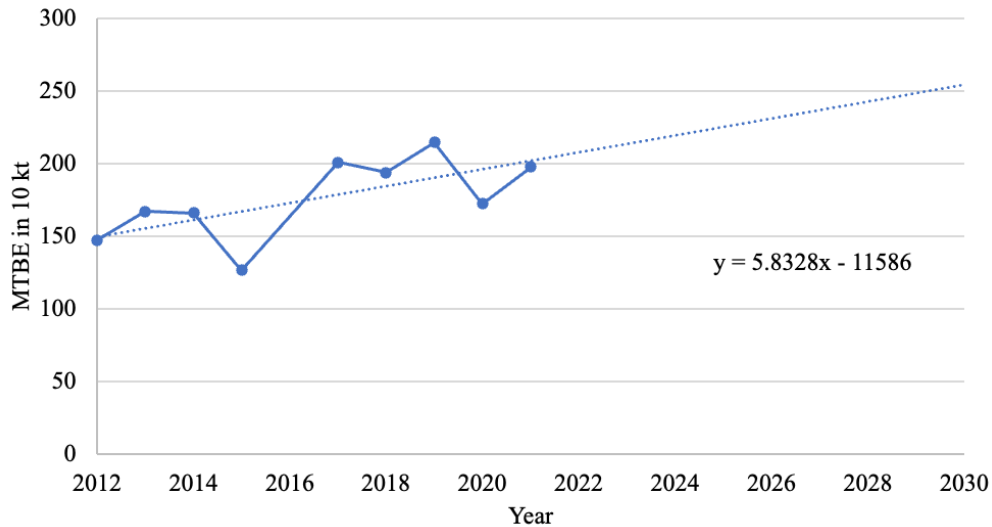


Figure 1.2. Extrapolated MTBE demand in CIS region, 2012-2021.

To forecast future demand, a linear regression model was employed using these historical data points. The trendline equation projects that the CIS demand for MTBE will reach approximately 2254.2 kt in 2025. Based on this value, the demand for the Kazakhstani market was estimated as 25% of the total CIS demand which was set to around 563.5 kt of MTBE per year. It was estimated that currently two plants in Kazakhstan are producing MTBE at a capacity of 77 kt/year [8].

Chapter 2. Process Summary

2.1. Process Description and PFD

Finalized process flow diagram (Figure 2.1) consists of these major units: 1 reactor and 3 separation columns. This model was adapted from several research and master thesis papers, where conventional MTBE production processes were considered [9,10,11].

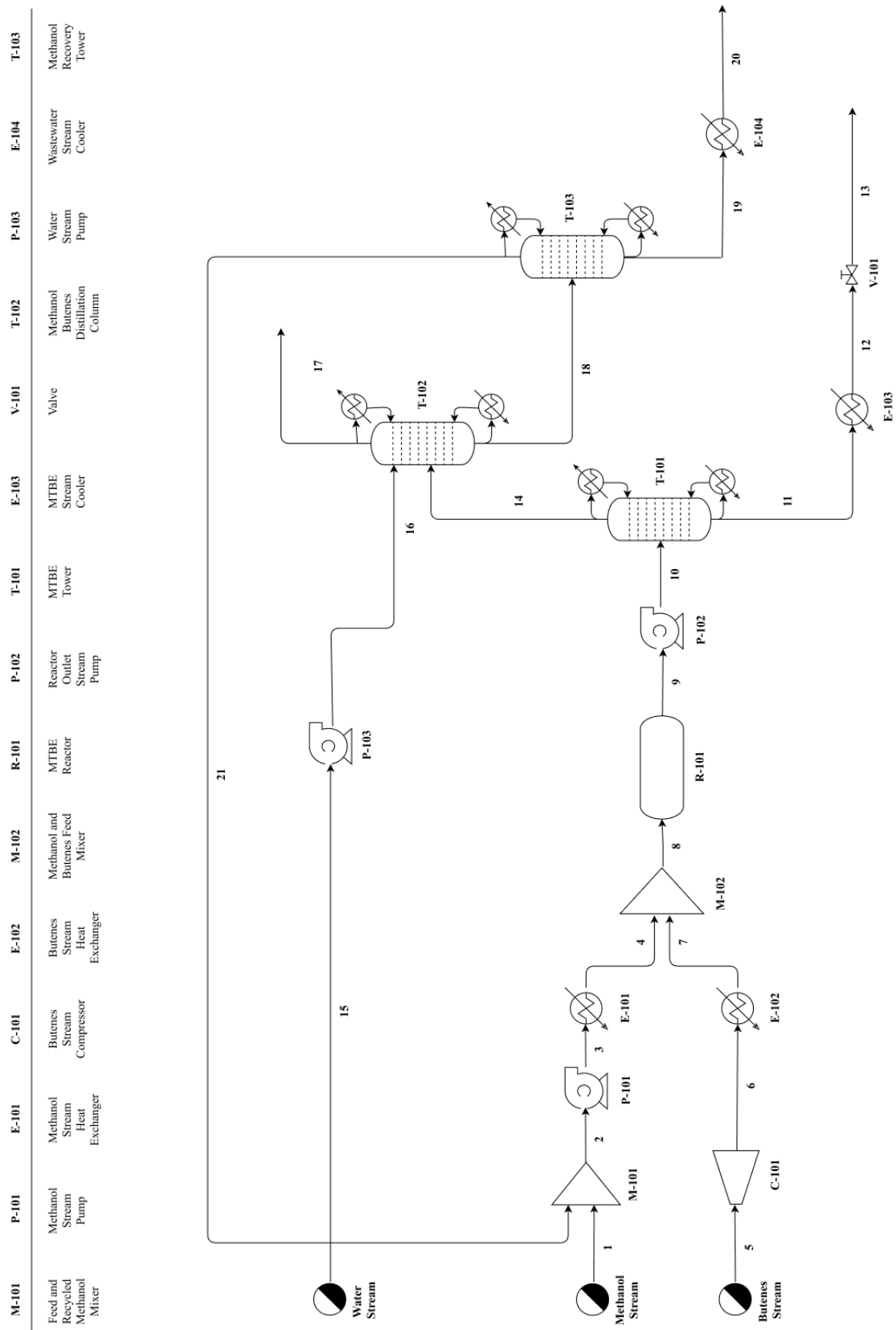


Figure 2.1. Process flow diagram.

Fresh liquid methanol (1) at 1 atm and 25°C is introduced into the system and fed to the mixer, M-101, where it combines with recycled methanol (21) from the distillation column, T-103. This mixing ensures the effective utilization of unreacted methanol from earlier process stages, reducing feedstock wastage. After mixing, the combined stream (2) at 1 atm and 29.6 °C is sent to the pump, P-101, which increases its pressure to 11 bar. The pressurized methanol (3) is sent to the heater, E-101, where temperature is increased up to 80°C for further mixing. This preheating step ensures that methanol is in a suitable state for mixing with the butenes stream. In parallel, a feed of isobutylene mixed with n-butenes in vapor phase (5) at 1 atm and 25°C is introduced to the compressor, C-101. The compressor raises the pressure of the butenes to 15 bar and as a result temperature of the stream becomes 125.887°C. This pressurized butenes stream (6) is sent to the cooler, E-102, where the temperature is decreased to 80°C, causing a phase change from vapor to liquid phase. The resultant butenes stream (7) exits the heater as a liquid and is sent further for mixing with methanol. Methanol (4) and butenes (7) streams are sent to the mixer (M-102), and the resulting combined feed stream (8) is at 11 bar and 79.5°C.

The combined stream (8), with a mole ratio of methanol to isobutylene of 1.34:1, enters a multi-tubular reactor, R-101. The reactor operates at 80°C and 11 bar and is designed as a heat exchanger: multi tubular packed bed PFR with catalyst being loaded in the tubes side. In the reactor, methanol and isobutylene react catalytically to synthesize the main product, MTBE. The reactor effluent (9), consisting of desired product, MTBE, along with unreacted methanol and isobutylene is directed to the first distillation column, T-101. MTBE of 96.4 % purity by mass is discharged from the bottom stream (11), and 2.5% of methanol by weight, which meets specifications set for MTBE product. Then, MTBE stream (11) is sent to the cooler, E-103, to decrease its temperature from 158.312°C to 25°C. Resulting stream (12) is directed to the valve, V-101, to reduce its pressure to 1.01325 bar to reach atmospheric pressure.

Fresh water stream (15) enters the system at 1 atm and 25°C and is pumped via P-102 up to pressure of 8 bar, which leaves the pump as stream 16. Both streams, 14 (butenes at 95.71°C) and 16, are introduced separately to the distillation column, T-102, where methanol is separated from butenes. From the top of the tower, butenes stream (17) with molar fraction of 0.837 (inerts plus IB) at 67.478°C and 7.92 bar is obtained.

The bottom product stream (18), consisting mainly of methanol and water, is sent to the next separation column, T-103, where methanol recovery occurs, and wastewater exits the system. The bottom product stream (19) is fed to cooler E-104, to reduce the temperature to 35°C. Then, wastewater stream (20) is discharged from the system and is going to be treated accordingly. The distillate stream (21) with 98.5% mole methanol at 64.437°C and 1.03 bar is recycled back for further processing. Recycled methanol stream (21) is combined with methanol feed (1) via mixer, M-101.

A more detailed stream temperature and pressure data could be traced in Tables 2.1 and 2.2 below.

Table 2.1. Temperature and pressure values for streams 1-11.

	Number of stream										
Property	1	2	3	4	5	6	7	8	9	10	11
Temperature, °C	25	29.560	30.147	80	25	125.887	80	79.523	79.523	79.863	158.312
Pressure, bar	1.01325	1.01325	11	11	1.01325	15	15	11	9.08	14	14

Table 2.2. Temperature and pressure values for streams 12-21.

	Number of stream										
Property	12	13	14	15	16	17	18	19	20	21	
Temperature, °C	25	25	95.710	25	25.213	67.478	156.224	114.011	35	64.437	
Pressure, bar	14	1.01325	13.7	1.01325	8	7.92	7.92	1.73	1.73	1.03	

2.2. Material Balance

The mass flow rates of each component and total stream for distillation columns' inlet and outlet streams are given in Tables 2.3, 2.4, 2.5, and 2.6.

Table 2.3. Mass balance for MTBE reactor R-101 with recycle.

Stream	Mixed Feed to Reactor	Reactor outlet
	8	9
IB, kg/hr	47971.223	34.790
Methanol, kg/hr	36654.427	9278.651
MTBE, kg/hr	9.045	75321.253
H ₂ O, kg/hr	21.970	21.970
Inerts (butenes), kg/hr	86882.302	86882.302
Total, kg/hr	171538.966	171538.966

Table 2.4. Total mass balance for T-101 column.

Stream	Feed to T-101	Bottoms (MTBE stream)	Distillate (MeOH+C ₄ s stream)
	10	11	14
IB, kg/hr	34.790	0.029	34.761
Methanol, kg/hr	9278.651	1585.858	7692.793
MTBE, kg/hr	75321.253	60217.236	15104.017
H ₂ O, kg/hr	21.970	4.774	17.196
Inerts (butenes), kg/hr	86882.302	645.192	86237.110
Total, kg/hr	171538.966	62453.089	109085.877

Table 2.5. Total mass balance for T-102 column.

Stream	Feed to T-102 (MeOH+C ₄ s stream)	Water Feed	Distillate (C ₄ 's out)	Bottoms (methanol-water)
	14	16	17	18
IB, kg/hr	34.761	0	34.761	0.0002
Methanol, kg/hr	7692.793	0	3436.430	4256.362
MTBE, kg/hr	15104.017	0	15094.980	9.037
H ₂ O, kg/hr	17.196	25942.003	372.145	25587.054
Inerts (butenes), kg/hr	86237.110	0	86209.964	27.146
Total, kg/hr	109085.877	25942.003	105148.280	29879.600

Table 2.6. Total mass balance for T-103 column.

Stream	Feed to T-103	Bottoms (wastewater)	Distillate (recycled MeOH)
	18	19	21
IB, kg/hr	0.0002	5.524E-10	0.0002
Methanol, kg/hr	4256.362	427.799	3828.650
MTBE, kg/hr	9.037	1.513E-07	9.045
H ₂ O, kg/hr	25587.054	25565.031	21.970
Inerts (butenes), kg/hr	27.146	4.833E-05	27.154
Total, kg/hr	29879.600	25992.830	3886.820

The composition of the MTBE produced is given in Table 2.7.

Table 2.7. Composition of the product by mass.

Stream	MTBE Stream
	13
IB	4.607E-07
Methanol	0.025
MTBE	0.964
H ₂ O	7.644E-05
Inerts (butenes)	0.010

It was specified that required target purity of MTBE is 96% with methanol content equal to or less than 2.5%, which is successfully achieved in the designed process.

Chapter 3. Major Equipment Design

3.1 Reactor R-101 Design

The main reaction in MTBE synthesis is given below in Fig. 3.1.:

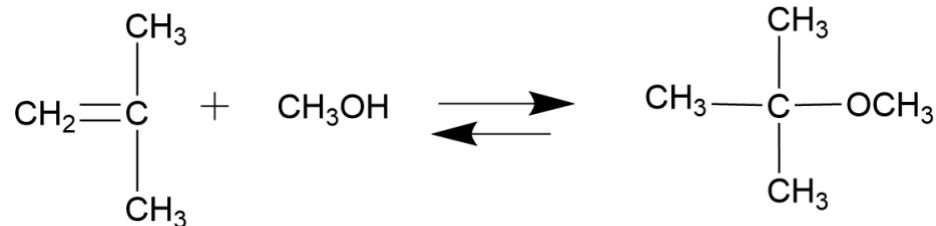


Figure 3.1. MTBE synthesis reaction.

The reaction is slightly exothermic and maintaining a constant temperature for high conversion and preventing catalyst deactivation is an important matter for the plant [12]. Therefore, the reactor is designed as a heat exchanger: multi tubular packed bed PFR with coolant water on the shell side. The catalyst is loaded in the tubes and cold water on the shell side is used to remove heat from the reaction and keep the temperature at 80°C throughout the reactor.

As the rate-determining step for the reaction is the surface reaction between adsorbed methanol and isobutylene, the reaction kinetics are modeled using Langmuir-Hinshelwood-Hougen-Watson (LHHW) mechanism for heterogeneous catalytic reaction [12]. The activity coefficients are used instead of concentration terms due to the nonideality of the liquids caused by their differences in polarities [12]. The upflow packed bed integral reactor system at 1.72 MPa (17.2 bar) was used for experiments in the reference paper, and the kinetic model is given below:

$$r = A_0 \exp\left(-\frac{E}{RT}\right) \left(\frac{\alpha_{IB}}{\alpha_{MeOH}} - \frac{1}{K} \frac{\alpha_{MTBE}}{\alpha_{MeOH}^2}\right) \quad (3.1)$$

where A_0 is a parameter with a value of $6.3 \cdot 10^{12}$ mol/(h*g), E is an activation energy (85.4 kJ/mol), α_{IB} , α_{MeOH} and α_{MTBE} are activity coefficients for isobutylene, methanol, and MTBE respectively [12]. K is an equilibrium constant given by equation below, where T is temperature in Kelvins [12]:

$$\ln K = -13.482 + 4388.7 T^{-1} + 1.2353 \ln T + 0.0879T \quad (3.2)$$

From the reaction kinetics it can be seen that rate is mostly inhibited by methanol [12]. This happens due to the fact that methanol has a considerably higher affinity than isobutylene for adsorption, displacing isobutylene from the catalytic surface, therefore reducing the reaction rate [12].

To verify the kinetics, the figure from the reference paper was reproduced using Aspen Plus v14 simulation. Inputs in simulation are: pressure of 1.72 MPa, MeOH to IB ratio of 1.05, 1 kg catalyst loading, reactor length and diameter of 10 and 0.2 m accordingly. The Figure 3.2 represents the conversion of IB as a function of space time (weight of catalyst divided by inlet flow rate of IB) at 333 K [12].

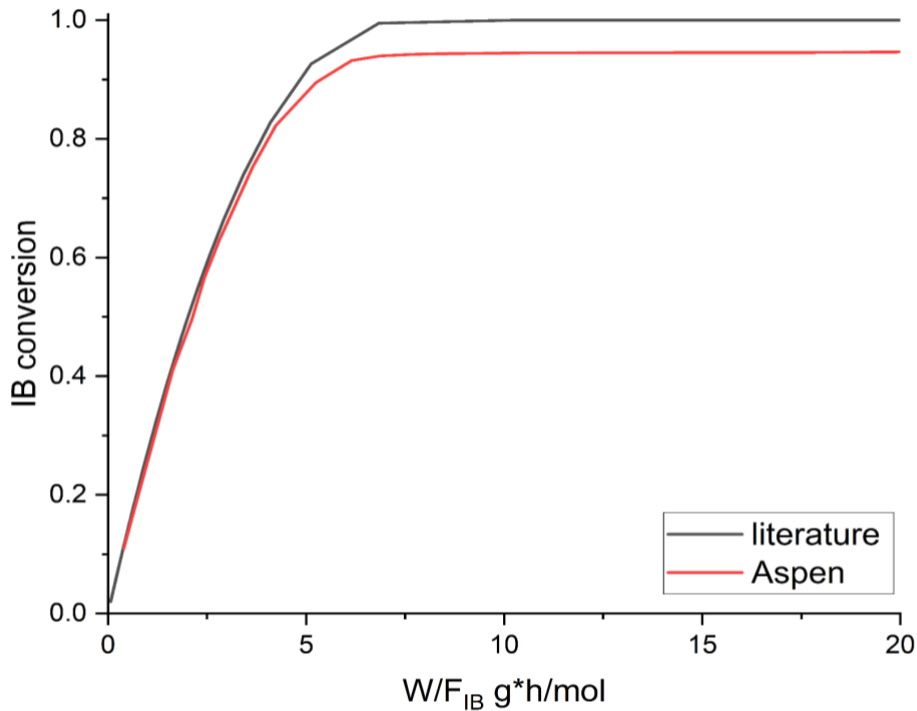
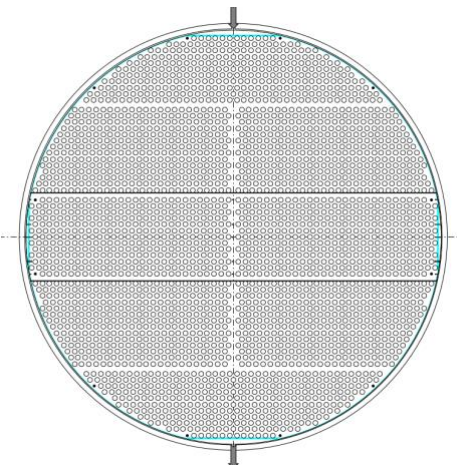


Figure 3.2. Simulation results and literature data for conversion of IB as a function of space time for 333 K [12].

The design for the dimensions of the unit was done using Kern's Method [13]. The design equations and assumptions are given in the ESI. The coolant flow rate was calculated using the heat duty of the reaction and heater unit in Aspen Plus V14, so that water inlet is at 25°C and outlet temperature is 60°C. The reactor specifications are given in Table 3.1. The triangular pitch was chosen to reduce the shell size and fit more tubes. The material selected for design is stainless steel ASTM 304. The selected steel is commonly used for tubes, has low carbon content, can be used for corrosive liquids, and has fairly high allowable stress, while being cheap [14,15]. Molar composition in the reactor is presented in the Appendix E.

Table 3.1. Reactor R-101 specification sheet.

Reactor, R-101	Type	Multitubular packed bed with coolant water	Orientation	Horizontal
Operating conditions				
	Shell	Tube		
Components	Coolant water	Isobutylene, methanol, MTBE, water, inerts		
Mass flow, kg/s	111.43	46.57		
Temperature, °C	25 to 60	80		
Pressure, bar	1	11		
Pressure drop, bar	0.064	1.838		
Overall heat transfer coefficient, W/m ² K	558.355			
Heat transferred, MW	19.58			
Dimensions				

Inner diameter, m	2.333	0.025	
Outer diameter, m	2.393	0.032	
Total number of tubes	3062		
Number of passes	8		
Length, m	4	3.66	
Reactor volume, m ³	17.2	5.5	
Material	Stainless steel TP304		
Catalyst			
Name	Amberlyst-15		
Catalyst loading, kg	3353.089		
Apparent density, kg/m ³	1010		
Shape	Spherical		
Average particle diameter, mm	0.74		
Average pore diameter, nm	28.8		
Packing density, g/cm ³	0.61		

3.2 Compressor C-101 Design

Since the reaction proceeds in liquid phase, the pressure of the reactants had to be increased to 15 bar. Based on the discharge pressure of 15 bar and inlet volumetric flow rate of 58789.4 m³/hour centrifugal compressor was chosen.

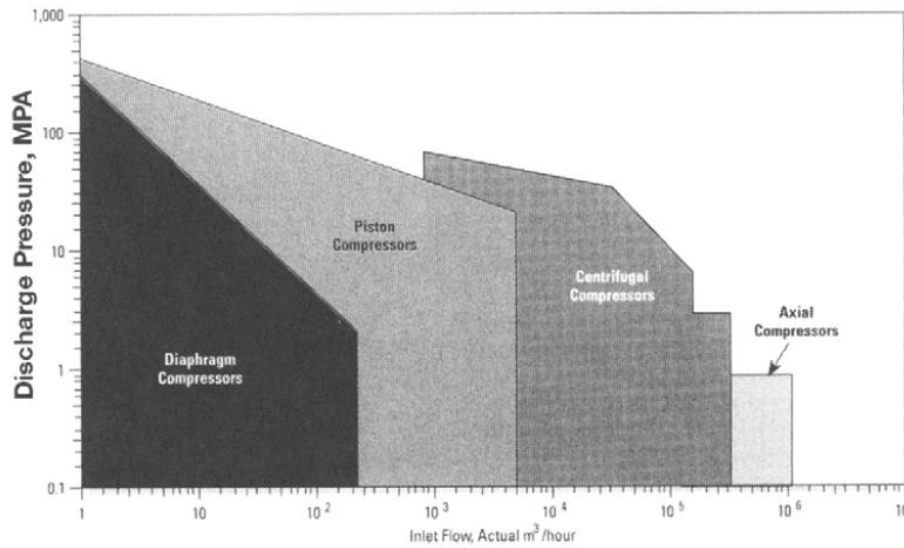


Figure 3.3. Approximate ranges of compressor types used in petrochemical industries [16].

The C-101 unit was chosen as a major equipment due to its importance, because it was preparing part of the reactants to enter the reactor, where the main reaction happens. Centrifugal compressor had to increase the pressure of butenes stream, which has volumetric flow rate of 16.33 m³/s from 1.01325 bar to 15 bar. Inlet and outlet conditions of the streams will be given in Tables 3.2 and 3.3 respectively.

Table 3.2. Feed properties of the C-101 compressor.

Parameter	Symbol	Unit	Value
Gas composition	Isobutylene (C ₄ H ₈ -5) 1-butene (C ₄ H ₈ -1)	-	0.3558 0.6442
Inlet pressure	P ₁	bar	1.01325
Inlet temperature	T ₁	°C	25
Inlet volumetric flow rate	V ₁	m ³ /s	16.33
Compressibility factor at the inlet	Z ₁	-	1

Table 3.3. Outlet properties of the C-101 compressor.

Parameter	Symbol	Unit	Value	
Outlet pressure	P_2	bar	15	
Outlet temperature	T_2	°C	138.95	125.89 (Aspen value)
Outlet volumetric flow rate	V_2	m ³ /s	1.52	1.48 (Aspen value)
Compressibility factor at the outlet	Z_2	-	1	

Compressor was assumed to operate polytropically with 80% efficiency, which is close to the real-world compressors in the industry. It was calculated that the single-shaft compressor will have 4 stages and will be able to provide 140 kJ/kg polytropic head with 6582 kW power requirements [17]. Latter 2 values were also validated by the Aspen Plus V14 simulations, but discharge temperature and volumetric flow rate differ slightly due to the usage of constant C_p and C_v , while in the Aspen Plus V14 simulations are done using variable C_p and C_v .

Main 3 parts of the compressor: impeller, diffuser and volute were designed thoroughly and suitable materials for their fabrication were chosen [18]. 3D-shrouded impellers, which were calculated to have the diameter of 933 mm and rotational speed of 5424 revolutions per minute, will be fabricated from 17-4PH Stainless Steel [19], which is an alloy mainly consisting of chromium, nickel, copper and iron. It has a high yield strength of 1100 MPa, because the impeller is the part which experiences the most stress out of all parts of the compressor. Alloy with chromium was also chosen in order to withstand corrosive properties of the gas as a precaution [20]. Diffuser, volute and casing will be fabricated from the ASTM 304 stainless steel [15]. All the calculated parameters will be given in Table 3.4. There were several assumptions made in order to ease the calculations, such as compressor efficiency as 80%, flow coefficient as 0.09 and ratio of hub and eye diameter as 0.6. All of those assumptions can be considered reasonable due to all of them being at an acceptable range of design.

Table 3.4. Compressor specifications.

Parameter	Symbol	Unit	Value
Polytropic head	y_p	kJ/kg	140.59

Number of stages	n_{stages}	-	4
Polytropic efficiency	η_p	-	0.8
Power requirements	P	kW	6581.9
Impeller specifications			
Number of impellers	n_{impeller}	-	4
Number of blades (on each impeller)	n_{blades}	-	18
Tip speed	u_2	m/s	265.14
Rotational speed	N	rpm	5424.7
Mach number at the tip	M_{u_2}	-	1
Impeller diameter	d_2	mm	933
Disk diameter	d_{20}	mm	971
Blade thickness	s	mm	9.71
Hub diameter	d_H	mm	327
Eye diameter	d_E	mm	545
Blade inlet diameter	d_1	mm	468
Impeller inlet width	b_1	mm	101
Impeller exit width	b_2	mm	47
Blade angle	β_{1B}	deg	22
Blade exit angle	β_{2B}	deg	50

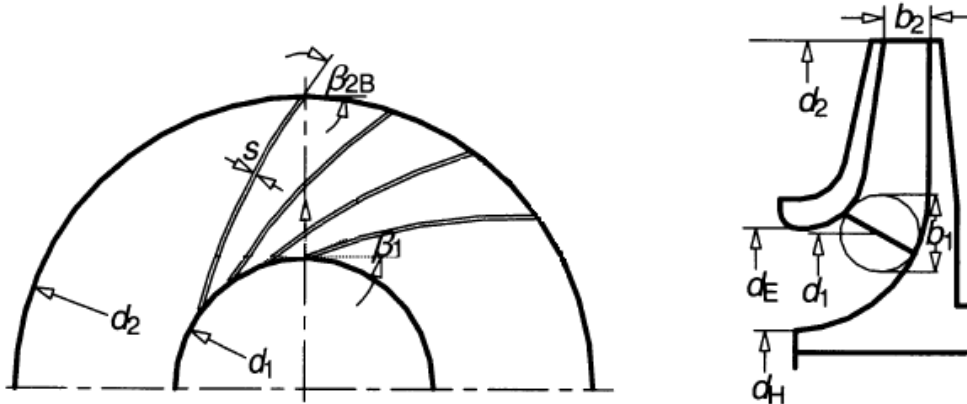


Figure 3.4. Impeller geometry. Subscripts: 1 blade leading edge midpoint, 2 blade trailing edge, E eye, H hub, B blade, b width [18].

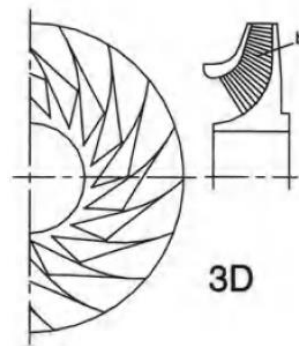


Figure 3.5. 3D-impeller, shrouded with twisted backward-curved blades, b straight-line blade elements for 5-axis NC flank milling [18].

Vaneless type diffuser

Diameter of diffuser inlet	D_{in}	mm	971
Diameter of diffuser outlet	D_{out}	mm	1700
Diffuser inlet width	b_{d2}	mm	258

Volute

Volute outer diameter	D_v	mm	1923
-----------------------	-------	----	------

Casing

Length	L	m	1
Height	H	m	2

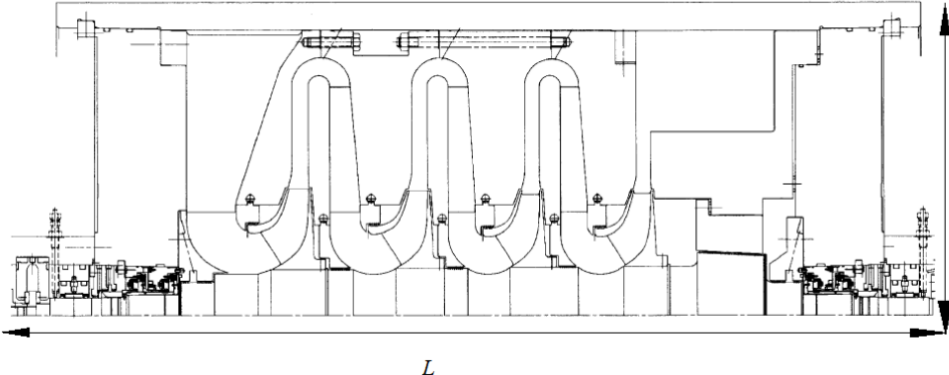


Figure 3.6. Single-shaft compressor with 4 impellers [18].

3.3 Heat Exchanger Design

3.3.1 Heat Exchanger E-101 Design

The main purpose of this unit is to heat fresh methanol stream mixed with recycled methanol stream, coming from T-103, from 29.6 °C to 80 °C. This is a preheating step before a methanol stream is fed to the reactor R-101, which operates at 80 °C and 11 bar. Before the methanol stream is heated, it is pumped to 11 bar in P-101, and then sent to E-101.

Heat exchanger E-101 is designed with one shell pass and two tube passes. Steam was assigned to the shell-side, as it is condensing, and methanol to tube-side, as it is highly corrosive [21]. As for material selection, we chose SS 316L as it is compatible with methanol and water. According to Industrial Specialties Mfg. and IS Med Specialties (ISM), methanol and water compatibility with this type of steel is marked as grade A (which is excellent) [22]. Also, SS 316L is relatively cheaper and widely used in industrial heat exchanger applications. As compared with a cheaper SS 304, the chosen material has better corrosion resistance, thus longer performance [14]. As for rear end head types, fixed head (Type M) was used as it is usually used for condensing streams [13].

Initially four tube passes were used, but as this arrangement increased tube-side velocity, which is not preferred at high flow rates, a change to two tube passes was introduced (one tube pass provided low velocity, which is not desired). Due to vibration warnings during Aspen simulations, it was decided to split a single heat exchanger to 5 heat exchangers in parallel to reduce velocity inside tubes and shells. As vibration warnings were still present, baffle spacing

was increased from 0.2 to 0.55 times of shell diameter, which resulted in errorless heat exchanger operation in Aspen. It is recommended that baffle spacing is 0.2-1.0 times of the shell diameter, and since initial guessing was not satisfactory some changes were introduced [13].

In the heating process condensation takes place in the shell-side and it was assumed that entering saturated vapor exits the heat exchanger as saturated liquid at isothermal conditions. Therefore, all the calculations were performed using equations for total condensation design. Since 5 shells in a parallel model were used, calculations were based on the flow rates divided by 5. All formulas used in calculations were taken from Heat-Transfer Equipment book [13].

Fluid properties (density, viscosity, thermal conductivity, heat capacity) of methanol stream for calculations were taken from stream results (add properties) at mean temperature. As water enters the shell-side as steam and leaves as a condensate, fluid properties at 1.9 for liquid and vapor were taken in the same manner respectively.

A comparative analysis of hand calculated and Aspen values is presented in Table 3.5 below.

Table 3.5. Comparison of hand calculated values and Aspen Plus V14 results.

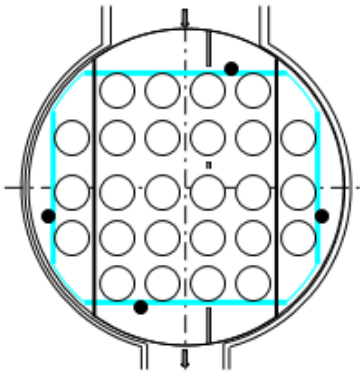
Parameter	Hand calculated	Aspen
Area, m ²	29.819	29.675
Heat duty, kW	1699.87	1693.64
Average heat transfer coefficient, W/m ² K	989.321	976.103

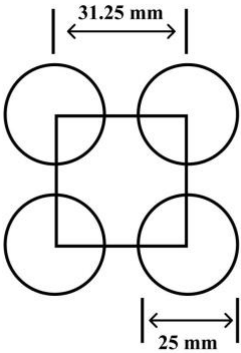

Since Aspen does not heat methanol stream to exactly 80°C, heat duty, area, and average heat transfer coefficient values obtained from simulation differ, but by a small margin of error. Also, previous assumption of total condensation of water steam at isothermal conditions was not fully performed by Aspen, as decrease of 2°C in temperature was observed, which may be assumed as almost negligible.

A specification sheet from Aspen Plus V14 with calculated input parameters is presented in Table 3.6 below.

Table 3.6. Specification sheet for E-101.

Heat Exchanger E-101		Function: preheating methanol stream for feeding reactor, R-101	
Area, m ²	29.675	Type	BEM, 1-2 shell and tube heat exchanger, horizontal

Performance				
Fluid allocation	Shell-side (hot fluid)		Tube-side (cold fluid)	
Fluid name	Hot steam		Methanol stream	
Mass flow, kg/hr	2750.4		36712.6	
Stream	In	Out	In	Out
Temperature, °C	118.66	116.71	29.60	79.82
Pressure, bar	1.9	1.81	11	10.94
Pressure drop, bar	0.086		0.061	
LMTD (corrected), °C	58.47			
Overall heat transfer coefficient, W/m ² K	976.103			
Heat duty, kW	1693.64			
Geometry Dimensions				
Tube pattern	90-Square			
Number of tubes, N _t	21			
Tube passes	2			
Tubes OD, mm	25			
Tube wall thickness, mm	1.7			
Tube length, m	3.66			
Pitch, mm	31.25			

Shell ID, mm	219.38	
Baffle type	Single segmental Vertical cut	
Baffle cut	25%	
Baffle spacing, mm	120.66	
		

Generally, most of the design specifications were optimized by running Aspen simulations by trial-and-error analyses, mainly based on optimal geometry values taken from Heat-Transfer Equipment book [13]. To minimize pressure drop, optimal baffle cut of 25%, tube length of 3.66 m, and square pattern was chosen. Tube outer diameter and wall thickness dimensions were taken from standard steel pipe sizing parameters, and by trial-and-error, the most appropriate parameters were selected to be 25 mm and 1.7 mm, respectively. Tube pitch is generally 1.5 times longer than outer diameter, and this calculation was included in our design.

TQ curve (Fig. F.1) is attached in Appendix F and shows that there is no temperature cross, which justifies the design parameter selection for heat exchanger. Sensitivity analysis was also performed to check how changes in inlet conditions of methanol stream (temperature) affect outlet conditions (pressure and temperature) of methanol stream, and if any errors in operation of the heat exchanger appear. All the figures were presented in Appendix F. For the inlet methanol stream temperature in the range 20-40°C, there is a very small decrease in the outlet pressure, which is not that critical for the reactor to operate.

3.3.2 Heat Exchanger E-102 Design

The primary role of heat exchanger E-102 is to condense a butenes mixture from 131.742°C to 80°C while simultaneously heating a counter-current fresh and recycled water stream from 25°C to 50°C before it enters a downstream unit. Before reaching E-102, the butenes stream is pressurized to 15 bar by compressor C-101. The changes made from the previous design include changing the final temperature of water from 75 to 50, and all the consequent design specifications.

E-102 features a single shell pass and two tube passes. The butenes mixture condenses on the shell side, while water flows through the tube side due to its high corrosiveness [21]. The

selected construction material is SS 316L, which is highly compatible with both butenes and water. Additionally, SS 316L is widely used in industrial heat exchangers due to its cost-effectiveness.

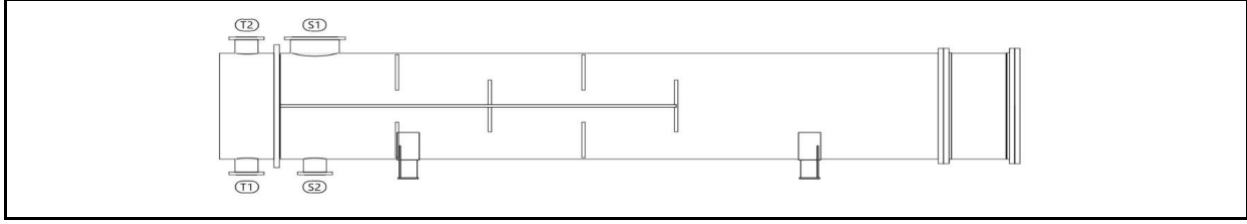
During Aspen simulations, vibration warnings were detected presumably due to higher mass flow rate due to shrunken temperature difference which resulted in higher pressure drop, and faster condensation of butenes. Measures taken to get rid of it included increasing baffle cut and shell diameter, decreasing fluid mass flow, increasing number of tubes, etc. However, all of this resulted only in a bigger deviance from expected thermal results. Thus, the priority for design specifications was to ensure the correct outflow temperature on each side.

For the calculations, fluid properties (density, viscosity, thermal conductivity, and heat capacity) of water were taken from stream results at the mean temperature. As the butenes stream undergoes phase change, properties for both vapor and liquid at 15 bar were determined based on wall temperature. Key parameters such as tube outside diameter, number of tubes, shell diameter, baffle spacing, and tube length were optimized through trial and error, following methods are described in the literature [23]. Detailed calculations are available in the appendix, along with supporting figures used in the analysis. The fluid properties used in the calculations were evaluated using mixture analysis in Aspen Plus V14 at the mean temperatures of each stream.

Table 3.8. Specification sheet for E-102.

Heat Exchanger E-102		Function: condensating butenes , E-102		
Area, m²	279.642	Type	DFL, 1-2 shell and tube heat exchanger, horizontal	
Performance				
Fluid allocation	Shell-side		Tube-side	
Fluid name	Isobutylene(35.58%) + 1-Butene(64.42%) Mixture		Water	
Mass flow, kg/s	37.45		137.45	
Stream	In Stream	Out Stream	In Stream	Out Stream
Temperature, °C	131.742	80	25	50
Pressure, bar	15	14.54	1	0.482

Pressure drop, bar	0.46	0.538
LMTD, °C	54.35	
Overall heat transfer coefficient, W/m ² K	946.581	
Heat transferred, kW	14364.3	
Geometry Dimensions		
Tube pattern	90-Square	
Number of tubes, N _t	976	
Tube passes	2	
Tubes OD, mm	19	
Tubes ID, mm	15.6	
Tube wall thickness, mm	1.7	
Tube length, m	4.88	
Pitch, mm	23.75	
Shell ID, mm	976	
Baffle type	Single segmental Horizontal cut	
Baffle cut	25%	
Baffle spacing, mm	680	



Most design specifications were confirmed by Aspen and additional literature [23]. Optimal design geometry was ensured by TEMA standards. It was used in order to obtain an initial guess of correct parameters, particularly, Tubes outer diameter, length and wall thickness. To ensure that there is not a temperature crossover, TQ curve was obtained and put in the appendix - Figure G.1.

3.4 Distillation Column Design

After completion of the reaction, the product stream is directed into distillation columns to separate the needed product (MTBE) from inerts and unreacted reagents. Calculations for distillation columns' specifications were performed using the Fenske-Underwood-Gilliland (FUG) correlations.

Relative volatility for the T-101 Distillation column was calculated by taking geometric mean of K-values from feed, top and bottom streams taken from Aspen Plus V14 and using the formula 3.3. For optimal separation of the components, heavy key was chosen to be MTBE, light key – butenes.

$$\alpha_{i/HK} = \frac{K_I}{K_{HK}} \quad (3.3)$$

The relative volatility for T-103 was calculated via Antoine's equation. The obtained saturation pressure of the light key (*MeOH*) in the distillate/bottom was divided by the saturation pressure of the heavy key (*H₂O*) in the distillate/bottom to get the relative volatilities. Then, the geometric mean of these values was taken.

$$\log_{10} P_{sat} = A - \frac{B}{C + T} \quad (3.4)$$

Fenske equation was used to calculate the minimum number of stages [24]:

$$N_{min} = \frac{\ln\left[\left(\frac{x_{LK}}{x_{HK}}\right)_D \left(\frac{x_{HK}}{x_{LK}}\right)_B\right]}{\ln[\alpha_{LK/HK}]} \quad (3.5)$$

where, $(x_{LK})_D$ – mole fraction of light key component in the distillate, $(x_{HK})_D$ – mole fraction of heavy key component in the distillate, $(x_{LK})_B$ – mole fraction of light key component in the bottom

stream, $(x_{HK})_B$ – mole fraction of heavy key component in the bottom stream, $\alpha_{LK/HK}$ – relative volatility of the light key component compared to the heavy key component.

Then, Underwood correlations were used to calculate the minimum reflux ratio [24].

$$R_{min} + 1 = \sum \frac{\alpha_{i,HK} * x_{i,F}}{\alpha_{i,HK} - \theta} \quad (3.6)$$

where, R_{min} – minimum number of stages, $\alpha_{i,HK}$ – relative volatility of chosen component relative to heavy key component, $x_{i,F}$ – mole fraction of component in feed, θ – root of equation.

$$1 - q = \sum \frac{\alpha_{i,HK} * x_{i,D}}{\alpha_{i,HK} - \theta} \quad (3.7)$$

where, q – quality of feed, $x_{i,D}$ – mole fraction of components in distillate.

Quality of feed q was calculated with the following formula [25]:

$$q = \frac{-H_F + H_V}{H_V - H_L} \quad (3.8)$$

where, H_F – enthalpy of feed stream, H_V – enthalpy of saturated vapor, H_L – enthalpy of saturated liquid

Enthalpy values were taken from Aspen Plus V14.

For both T-101 and T-103 distillation columns, q was taken as 1, because enthalpy of feed and enthalpy of saturated liquid were found to be the same.

Then the value of θ was determined using Goal-Seek feature in Excel, and then the value of R_{min} was calculated using eq. (3.6). R was approximated to be 1.5 times the R_{min} value according to the heuristics [26].

Thus, Gilliland correlations were used to calculate actual number of stages [24]:

$$\psi = \frac{R - R_{min}}{R + 1} \quad (3.9)$$

where, R – reflux ratio.

$$\frac{N - N_{min}}{N + 1} = 1 - \exp\left(\frac{1 + 54.4\psi}{11 + 117.2\psi} \times \frac{\psi - 1}{\psi^{0.5}}\right) \quad (3.10)$$

where, N – number of actual stages.

Then N_{feed} was calculated using Kirkbride's equation [24]:

(3.11)

$$\frac{N_{above}}{N_{below}} = \left[\left(\frac{x_{HK,F}}{x_{LK,F}} \right) \left(\frac{x_{LK,B}}{x_{HK,D}} \right)^2 \left(\frac{B}{D} \right) \right]^{0.206}$$

where, N_{above} – number of stages above the feed, N_{below} – number of stages below the feed, B – mole flow rate of bottom stream (kmol/hr), D – mole flow rate of distillate stream (kmol/hr).

As for the material of the columns, 316L stainless steel was chosen because of its corrosion resistance, compatibility with the used components and high temperature strength [15]. According to Peters et al. [15], this material is suitable for distillation columns, specifically for welded construction, which is our case exactly.

3.4.1 Distillation Column T-101 Design

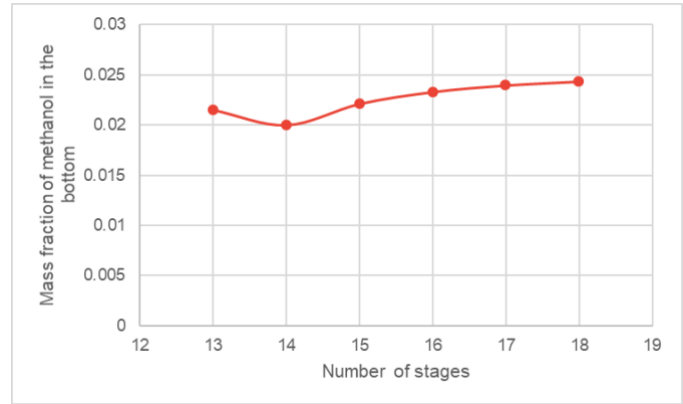
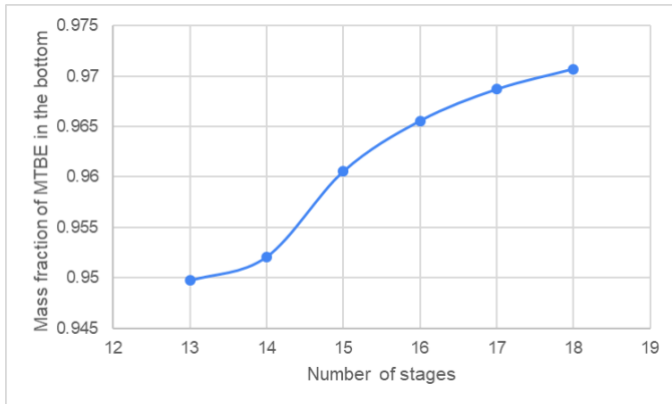
Reactor output stream, which consists of butenes, MTBE, methanol, IB and water (in descending order of their molar fractions in the feed), was fed to T-101 distillation column to separate MTBE in the bottom stream from other components in the distillate stream. This was performed according to the state standard “ST RK 2533-2021” [27], which states that the product of grade B should contain at least 96% of MTBE, at most 2.5% of methanol and 1.5% of butenes (all by mass). Results of hand calculated FUG calculations were shown in Table 3.9 along with the detailed calculations in the Excel file.

Table 3.9. Hand calculated variables.

N_{min}	N	N_{feed}	R_{min}	R
4.748	10.206	2.117	0.6915	1.0372

After completing hand calculations, these parameters were put into DSTWU equipment in Aspen Plus V14 to validate the results. However, these values did not yield needed MTBE, methanol and butenes mass composition in the resulting stream. This can be explained by the fact that this process is a multicomponent distillation, which is much more complicated than binary distillation due to possible chemical reactions and azeotrope formations, meaning that their deviations from ideal behavior are that much more significant [24]. FUG correlations constitute a shortcut method of approximating column parameters assuming ideal mixture behavior. Therefore, deviations between hand calculations and resulting values from DSTWU can be seen as acceptable.

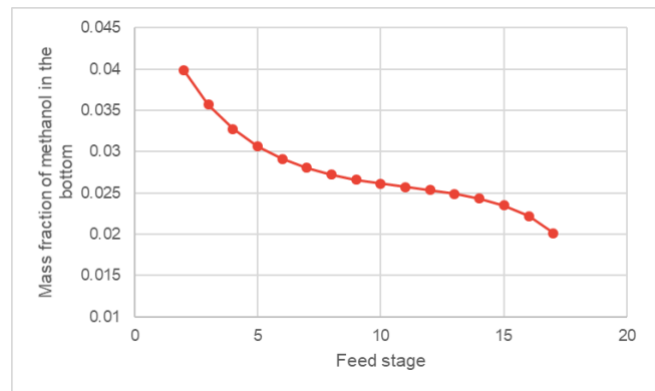
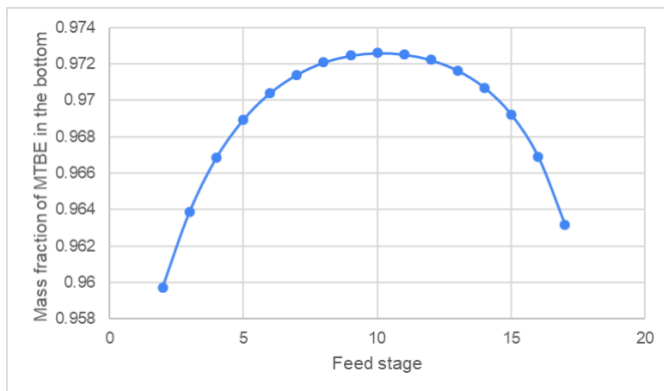
Then, Radfrac equipment was utilized to achieve needed mass compositions by applying several sensitivity analyses on distillate rate, number of stages, feed stage, reflux ratio and pressure of the column, which are shown in Figures 3.7a, 3.7b. It was necessary to pick the optimal values of the aforementioned parameters so that the mass fraction of MTBE in the bottom was no less than 0.96 as well as mass fraction of methanol no more than 0.025.



Figures 3.7a, 3.7b. Sensitivity analysis: Number of stages vs. Mass fraction of MTBE in the bottom.

18 stages were chosen as they yielded the highest MTBE mass fraction while keeping the methanol one under 0.025.

By observing Fig. 3.8a, 3.8b, it is evident that at feed stage 10 the mass fraction value of MTBE is the highest of 0.9726, however it cannot be chosen as the same feed stage yields the value of 0.026 for methanol. Thus, feed stage 14 was selected.



Figures 3.8a, 3.8b. Sensitivity analysis: Feed stage vs Mass fraction of MTBE in the bottom.

Figures 3.9a and 3.9b demonstrate the relationship between reflux ratio of the column with mass fractions of MTBE and methanol. Reflux ratio of 4 was chosen to ensure stability of MTBE purity and to keep MTBE losses in the distillate as low as possible, improving process efficiency and yield.

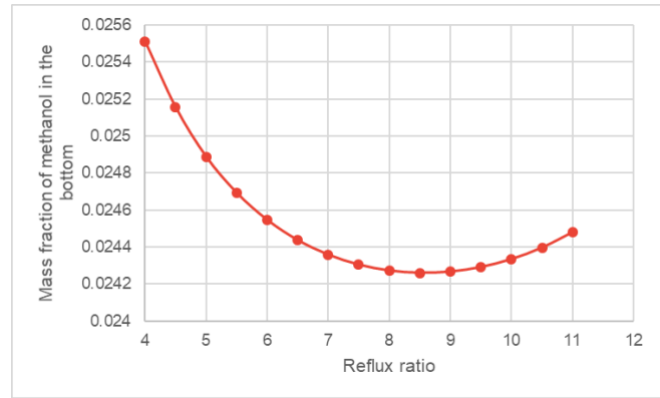
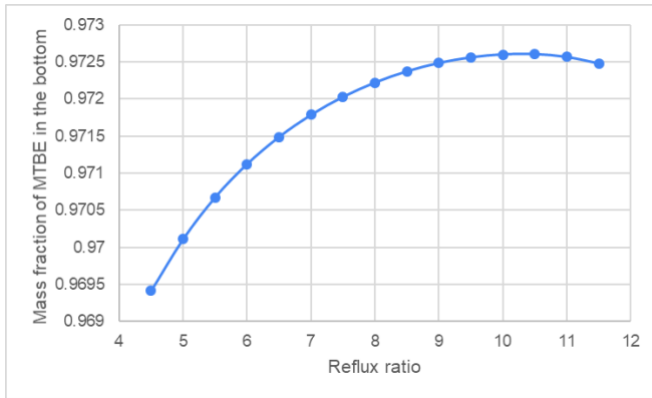
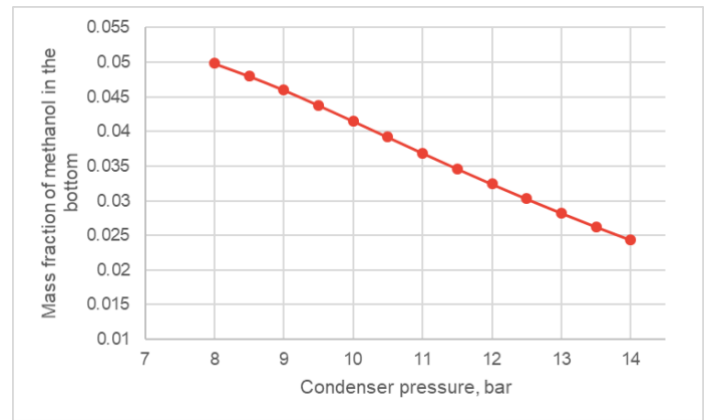
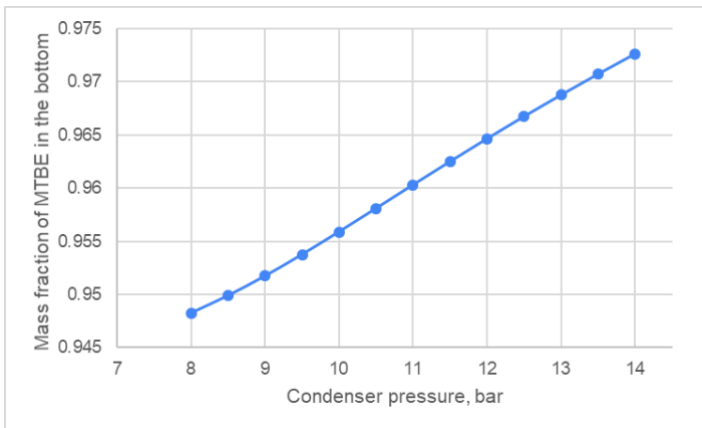


Figure 3.9a, 3.9b. Sensitivity analysis: Reflux ratio vs. Mass fraction of MTBE in the bottom.

As for the Figures 3.10a and 3.10b, condenser pressure of 14 bar was chosen as it is the minimum pressure that results in needed methanol fraction in the bottom stream.



Figures 3.10a, 3.10b. Sensitivity analysis: Condenser pressure (bar) vs Mass fraction of MTBE in the bottom.

After building and specifying the Radfrac column at equilibrium conditions, its internals were then specified and edited to obtain correct hydraulic plots without warnings. After that the column calculation type was changed to rate-based, according to changes were made and internals once again corrected to yield functional hydraulic plots. The resulting column dimensions are specified in Table 3.10 below.

Table 3.10. Distillation Column T-101 specifications.

Distillation Column T-101	Function: separation of needed product
Internal Conditions	

	Temperature, °C	Pressure, bar	Mole flow, kmol/hr
Feed	79.749	14	2694.38
Distillate	95.710	13.7	1950
Bottom	158.312	14	744.38

Operating Conditions

Column height, m	15.68	
Column diameter, m	5.7	
Condenser type	Total	
Reboiler type	Kettle	
Number of stages	18	
Number of trayed stages	16	
Feed stage	14	
Reflux ratio	4	
Construction material	Stainless steel 316L	

Technical data

Stage 1 (2-17 stages)

Tray type	SIEVE	
Tray spacing, m	0.98	
Hole diameter, m	0.0127	
Weir height, m	0.0817	

Weir length, m	5.694	
Side weir length, m	2.892	
Downcomer width top, mm	394.1	
Downcomer width bottom, mm	394.1	

Having run the Aspen simulation, composition, and temperature profile plots available in Appendix H [H.1, H.2] were obtained.

The composition profile plot demonstrates the way concentration of heavy (MTBE) and light key (butenes) components varies along the column stages. A well-defined separation is observed when there is a steep change in composition between the stages, indicating that the column is effectively separating the components. Resulting mole fractions align with the needed composition, achieving the goal of this column.

The temperature profile plot of the distillation column T-101 shows a gradual decrease in temperature from the bottom to the top of the column. This is expected, as the reboiler at the bottom provides heat to vaporize the components, while the condenser at the top removes heat to condense the lighter fractions. A smooth and steady temperature gradient across the column trays indicates efficient separation.

3.4.2 Distillation Column T-103 Design

The bottom stream of the T-102 column, which mainly consists of a methanol-water mixture, is transferred into the T-103 distillation column to separate the mixture and purify methanol, which will go back to the reactor as a recycle stream. This step is aimed at achieving the most effective separation of methanol from water to obtain higher methanol purity.

Table 3.11. Hand-calculated variables.

N_{min}	N	N_{feed}	R_{min}	R
10.578	17.954	4.917	4.343	6.515

The FUG method was initially used to estimate the parameters of the T-103 distillation column because it provides a quick and simplified approach for determining column specifications under the assumption of ideal mixture behavior. This method gives parameters like the number of stages, the reflux ratio, etc. After that, they were validated in Aspen Plus software. However, some differences were observed between the FUG calculations and the DSTWU results. Given that FUG correlations assume ideal mixture behavior, these deviations are acceptable.

Then, the Radfrac column was used to achieve the desired mole fractions by conducting multiple sensitivity analyses on key parameters, including distillate rate, number of stages, and feed stage. It was important to determine the optimal values for these parameters to maximize the mole fraction of MTBE in the distillate.

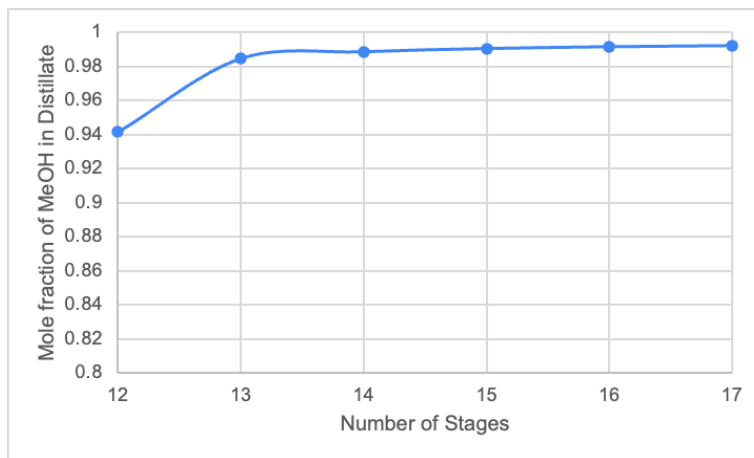


Figure 3.11. Sensitivity analysis: Number of stages vs. Mole fraction of MeOH in the distillate.

17 stages were chosen as they yielded the highest MTBE mole fraction as shown in Figure 3.11.

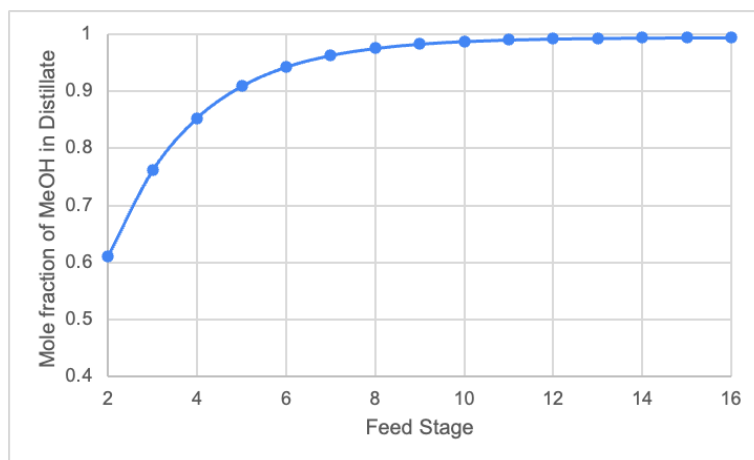


Figure 3.12. Sensitivity analysis: Feed stage vs. Mole fraction of MeOH in the distillate.

By observing the Figure.3.12, it can be seen that 11th -16th feed stages give the purest MeOH, however 12th feed stage was taken, giving 0.992 MeOH mole fraction in the distillate.

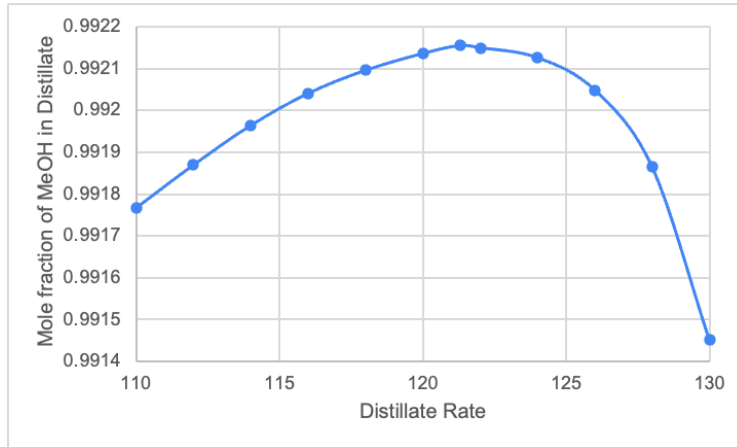


Figure 3.13. Sensitivity analysis: Distillate rate vs. Mole fraction of MeOH in the distillate.

Figure 3.13 demonstrates that the distillate rate exhibited an optimal point around 121.294 kmol/hr, beyond which we can see the decrease in the methanol purity.

The distillation column specifications are provided in Table 3.12 below.

Table 3.12. Distillation Column T-103 specifications.

Distillation Column T-103		Function: Purification of methanol	
Internal Conditions			
	Temperature, °C	Pressure, bar	Mole flow, kmol/hr
Feed	156.224	7.92	1553.72
Distillate	64.437	1.03	121.294
Bottom	114.011	1.73	1432.426
Operating Conditions			
Column height, m	11.25		
Column diameter, m	2.7		
Condenser type	Total		

Reboiler type	Kettle	
Number of stages	17	
Number of trayed stages	15	
Feed stage	12	
Reflux ratio	9	
Construction material	Stainless steel 316L	

Technical data

Stage 1 (2-16 stages)

Tray type	BUBBLE-CAP	
Tray spacing, m	0.75	
Hole pitch, m	0.038	
Weir height, m	0.063	
Weir length, m	1.889	
Side weir length, m	1.889	
Downcomer width top, mm	406.837	
Downcomer width bottom, mm	406.837	

The composition profile plot for the T-103 distillation column, available in Appendix (Figure I.1), illustrates the distribution of the heavy key component (water) and the light key component (methanol) across the column stages. Methanol remains dominant in the upper stages, while water concentrates toward the bottom, reflecting effective separation. A distinct shift in composition is observed at the feed stage (stage 12), where the introduction of the mixture causes a temporary disturbance. However, the overall trend confirms that the column successfully achieves the desired separation, ensuring a high-purity methanol product in the distillate.

The temperature profile, available in Appendix (Figure I.2), follows a trend, with temperatures increasing from the top to the bottom. This behavior aligns with the expected separation process, where the reboiler supplies heat to vaporize components, and the condenser cools the lighter fractions. Methanol, as the light key component, remains concentrated in the upper stages, while water, the heavy key, accumulates in the lower stages. A slight disturbance is observed at stage 12, where the feed is introduced, but the overall temperature gradient remains stable, indicating efficient separation.

Chapter 4. Minor Equipment Design

4.1 Distillation Column T-102 design

The bottom stream of the column T-101 and the water stream enter the column to separate butenes from the water and methanol mixture. The RadFrac unit was used in Aspen Plus V14 to model the design of the column. Specifications are given in Tables 4.1 and 4.2.

Table 4.1. Distillation Column T-102 specifications.

Number of stages	8
Feed (above-stage)	3
Condenser	Total
Reboiler	Kettle
Reflux ratio	10
Condenser pressure, bar	7.92
Pressure drop, bar	0

Table 4.2. Distillation Column T-102 specifications.

Condenser		Reboiler	
Temperature, °C	67.33	Temperature, °C	156.32
Heat duty, MW	-119.84	Heat duty, MW	121.539
Distillate rate, kmol/hr	1836.28	Bottoms rate, kmol/hr	1553.72
Reflux rate, kmol/hr	18362.8	Boilup rate, kmol/hr	12042.793
Reflux ratio	10	Boilup ratio	7.751

4.2 Heaters and Coolers Design

Since E-101 and E-102 were designed as major units, only E-103 and E-104 will be considered in minor equipment design. Heat duties of these units were calculated using mixture properties and applying the 5-point trapezoidal rule. Calculations will be provided in the ESI.

Table 4.3. Cooler specifications.

Cooler	ΔT , °C	Heat duty, kW (Aspen)	Heat duty, kW (by hand)
E-103	-134.48	-6533.48	-6538.21
E-104	-79.01	-2501.2	-2502.5

4.3 Pumps and Valves Design

Pumps are used to increase the pressure of the liquid going to the reactor and distillation columns. Pumps and valve specifications are given in Tables 4.4 and 4.5, respectively.

Table 4.4. Pump specifications.

Pump	ΔP , bar	Net work, kW (Aspen)	Net work, kW (by hand)
P-101	9.987	16.173	16.172
P-102	4.920	49.671	49.669
P-103	6.987	6.332	6.332

Table 4.5. Valve specifications.

Valve	ΔP , bar
V-101	-12.987

4.4 Storage Tanks Design

4.4.1 MTBE Storage Tank Design

After production, MTBE needs to be stored in tanks for sale. It was assumed that MTBE would be stored for 7 days, and 20% excess volume was assumed, which leads to a storage tank having a volume of 17073.5 m³. As this volume is too large it is divided into 30 tanks.

$$V_{MTBE} = 84.69 \frac{m^3}{hr} * 24 \frac{hr}{day} * 7 day * 1.2 = 17073.5 m^3$$

Table 4.6. MTBE storage tank specifications.

Construction material	ASTM 304 Stainless steel
Tank diameter, m	10
Tank height, m	10

4.4.2 Methanol Storage Tank Design

It was assumed that methanol would be stored for 15 days, as it was planned to buy it from the Chinese market, and 20% excess volume was assumed, which leads to a storage tank having a volume of 17884.8 m³. As this volume is too large it is divided into 30 tanks.

$$V_{MeOH} = 41.4 \frac{m^3}{hr} * 24 \frac{hr}{day} * 15 day * 1.2 = 17884.8 m^3$$

Table 4.7. Methanol storage tank specifications.

Construction material	ASTM 304 Stainless steel
Tank diameter, m	10
Tank height, m	10

Chapter 5. Plant Location and Layout

5.1 Plant Location

The choice of plant location was justified based on the following factors: availability of raw materials; geographical factors and infrastructure; governmental policies & economical considerations. Based on all of these factors, Kyzylorda region was selected, particularly “Öndiris” Industrial Zone (IZ).

5.1.1 Raw materials

Siting decision of the plant was based on availability of the raw materials and utilities. For our process, raw materials are methanol, water, liquified petroleum gases (LPG-s) and catalyst for Amberlyst 15. Based on economic considerations, it was decided to source methanol and Amberlyst 15 from China [27]. Since the Kyzylorda region is located in the southern part of Kazakhstan, it is more logistically efficient and cost-effective to transport it there, compared to other common industrial regions, such as Atyrau (Western Kazakhstan) and Pavlodar (North-Eastern Kazakhstan). Both process and utility water is going to be sourced from the nearby river Syr Darya, whereas LPG-s are going to be bought from the local refinery. Since the chosen site is located near both to the railroad and a river (see Fig. 5.1), it was considered the optimal choice.



Figure 5.1. Plant location.

5.1.2 Geographical Factors and Infrastructure

Local climate and weather conditions play a crucial role in selecting the site. Kyzylorda region has arid and highly continental climate with hot summers and relatively warm winters [28]. Minimal rain- and snowfall suggest year-round construction and operation with minimum weather-related downtime.

Geographically, the site is located on relatively flat and undeveloped land, which simplifies construction works. Closeness to Syr Darya river provides the opportunity to source water for the process and utility usage. Additionally, close proximity to Kyzylorda city ensures availability of skilled labor as well as needed services for construction and other long-term operations.

As can be seen from Fig. 5.1, a glass producing plant is also located in this area, suggesting that essential utility infrastructure already exists there, which can be potentially extended to support our plant as well. From the infrastructural point of view, the nearby railway line presents a great asset for transporting raw materials and exporting the end product.

5.1.3 Governmental Policies & Economical Considerations

“Öndiris” IZ was chosen for plant construction as it is a special territory equipped with communications and engineering and infrastructure, established according to the legislation of Republic of Kazakhstan [29]. Regarding the benefits and preferences of IZ, projects operating in this territory are exempted from both land and property tax. Moreover, after concluding an investment contract with the Investment Committee of the Ministry of Foreign Affairs of the Republic of Kazakhstan this project can be further exempted from customs duties, and simplified procedures for attracting foreign labor can be provided [29].

Regarding the market proximity, this region is located near several CIS countries, for instance, Uzbekistan, Kyrgyzstan and Turkmenistan. This geographic advantage facilitates shorter transportation distances, enabling efficient distribution of MTBE to neighboring fuel markets. Additionally, the presence of railway infrastructure in the area further supports cost-effective and reliable logistics for bulk transport across borders.

5.2 Plant Layout

The MTBE production plant is strategically designed to ensure the efficient and safe placement of all units, utilities, and administrative facilities. The plant is located adjacent to the Syr Darya river, giving an easy access to the process and cooling water, and is bordered by an already existing railway for the convenient transportation of raw materials and final products.

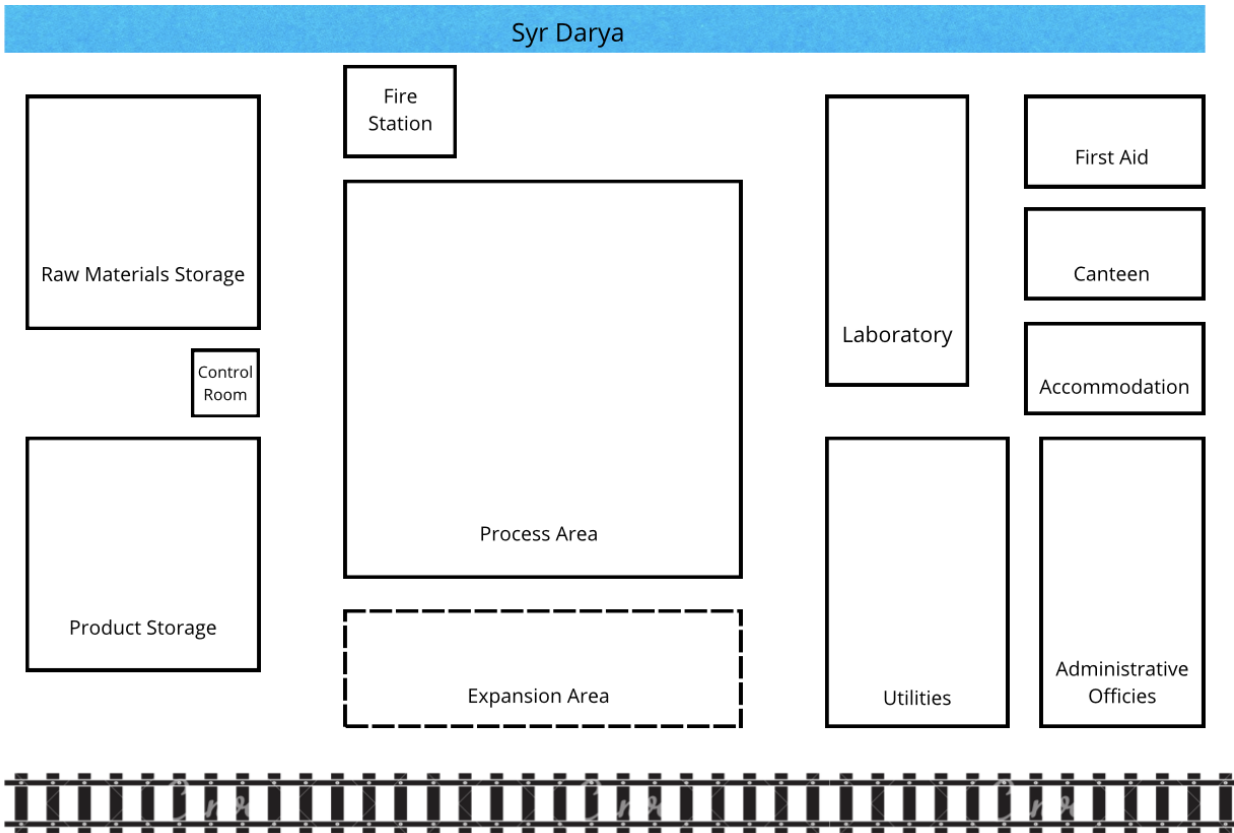


Figure 5.2. Plant layout.

5.2.1 Main Process and Storage Facilities

The process area occupies the central section of the layout, so that pipeline distances are minimized and to enhance the overall efficiency, additional expansion area is reserved nearby to accommodate future increases in production rates. A control room is placed adjacent to the process area to effectively monitor plant operations. The tank farm with raw materials is located near Syr Darya river since the process water is sourced from there. Moreover, taking into account the flammability risks associated with methanol and liquified petroleum gases, the storage area is located at a safe distance from the administrative offices, canteen and accommodation zones in case of leak or fire. Additionally, the tank farm with MTBE is located next to the railway line, to ease the transportation of the product for further selling purposes.

5.2.2 Emergency Facilities

A fire station is located near the Syr Darya river to ensure immediate access to water sources in case of emergencies. Furthermore, its strategic position near the process area and the storage tanks with flammable raw materials enables instant response to fire hazards. A first aid station is placed near administrative offices and accommodation areas to provide healthcare services for employees.

5.2.3 Laboratory and Utilities

The laboratory, which handles the analysis of raw materials, intermediate and final products to ensure their compliance with quality specifications, is located near the process area. The Utilities block is strategically positioned close to the electrical lines previously installed by the sheet glass plant, allowing for potential integration or simplified connection to the existing power infrastructure.

5.2.4 Administrative and Personnel Areas

The administrative offices are located farthest from the main process area and storage tanks to ensure the safety of workers and visitors. Adjacent to it, canteen and accommodation zones are situated to provide convenience and comfort for plant personnel.

Chapter 6. Environment and Waste Streams

In the MTBE production process, there are overall 3 outlet streams: 13, 18, and 20. 13 is the MTBE stream, which will be kept in a storage tanks and then sold. The other 2 streams will be discussed separately below.

6.1 Butenes Stream Treatment

18 is the butenes waste stream, which is a mixture of different gases. Its flow rate is 188.07 m³/hour, and it is 100% vapor. Composition of this stream will be given in Table 6.1.

Table 6.1. Composition of stream 18.

Compound	Mass fraction
MeOH	0.034
Isobutylene	0.0003
MTBE	0.137
Water	0.003
1-butene	0.825

Since the purity of the isobutylene and 1-butene for selling purposes was low, it was decided to use this stream for heat integration. From the Aspen Plus V14 software value of the HHV-15 parameter was computed and multiplied by the volumetric flow rate of this stream. It has been computed that 6.21 MW of energy can be integrated into the other energy-demanding equipment.

6.2 Wastewater Stream Treatment

Stream number 20 mainly consists of water and methanol, with a very small concentration of MTBE, isobutylene, and 1-butene. Composition of stream 20 will be given below in Table 6.2.

Table 6.2. Composition of stream 20.

Compound	Mass fraction
MeOH	0.015
Isobutylene	1.10×10^{-5} ppb
MTBE	0.00591 ppb
Water	0.985
1-butene	1.36 ppb

Since the concentration of isobutylene, MTBE, and 1-butene is low, only the environmental effect of methanol needs to be studied. According to Ullmann's Encyclopedia of Industrial Chemistry, methanol is readily biodegraded [30], but its concentration in wastewater is too high, around 13284.9 mg/L, which can damage the aquatic ecosystem. Concentrations above LOEC (47.49 mg/L) can damage food chains and retard growth and reproduction of fish. According to Kaviraj et al. [31], the NOEC value is 23.75 mg/L; therefore, methanol concentration has to be reduced at least to this value before discharge into the environment.

To reduce the concentration of methanol, stream 20 would be treated with activated sludge. Activated sludge was chosen because methods like air stripping or activated carbon were not suitable for industrial processes and a relatively low concentration (1.5%) of methanol [32]. The mechanism of wastewater purification is based on the activity of the biomass in the sludge. To put it simply, aerated microorganisms rapidly consume methanol, resulting in its lower concentration. These microorganisms utilize methanol as a carbon and energy source, converting it into less harmful byproducts like carbon dioxide and water, while simultaneously growing and forming settleable flocs that are then separated from the treated effluent. Monitoring of the treated effluent will be crucial to ensure the final methanol concentration meets the target NOEC and environmental regulations, which is between 10 and 50 mg/L before its discharge [33].

Chapter 7. Total Investment and Profitability

7.1 Cost of Equipment

The major equipment cost was calculated manually using the data and equations presented in the Chemical Engineering Design book [34]. More detailed calculations are provided in the ESI. For a minor equipment cost, Aspen Process Economic Analyzer (APEA) software was used to

roughly estimate the price. Since the software gives present values, only the location factor was considered. Calculated equipment and installation costs are summarized in Table 7.1.

Table 7.1. Equipment and installation costs.

Equipment	Unit	Equipment Cost, \$	Installation Cost, \$
Reactor	R-101	658,318.21	1,956,733.11
Heat exchangers	E-101	60,152.28	178,791.89
	E-102	146,569.34	435,651.13
	E-103	68,800.00	165,261.05
	E-104	31,400.00	110,315.57
Compressor	C-101	11,333,159.68	24,061,278.32
Pumps	P-101	27,900.00	73,713.56
	P-102	26,500.00	101,738.31
	P-103	8,500.00	46,962.67
Towers	T-101	4,356,624.51	12,694,423.68
	T-102	5,263,200.00	6,916,845.97
	T-103	375,849.98	998,698.85
	Total	22,354,315.92	47,732,513.46

Cost of the equipment was calculated by using the following formula (Eq. 7.1) by adjusting the parameters depending on the equipment being targeted:

$$C_e = a + bS^n \quad (7.1)$$

where C_e - purchased equipment cost on a US Gulf Coast basis (2010). USD; a, b - cost constants taken from the book [34]; S - size parameter; n - exponent.

Carbon steel was used as the reference material for all equipment cost estimations. After completing the initial calculations, the costs were adjusted to reflect the use of metal alloys (stainless steel 316L for most equipment and nickel for the compressor) while also accounting for inflation. This approach was consistently applied across all equipment to ensure accurate and up-to-date cost estimations.

Since the numbers taken for calculations were based on the US Gulf Coast, the location factor was chosen relative to China (indigenous), with a base value of 0.61. As this factor increases by 10% for every 1000 miles from an industrial area, and the closest Chinese industrial center (Sichuan [35]) is approximately 2,296 miles from Kyzylorda, the location factor was adjusted accordingly. Based on this distance, the location factor was calculated to be 0.75. Taking into account the exchange rate of yuan to USD, 1 yuan = \$0.121 (2003) [36] and 1 yuan = \$0.137 according to Wise exchange rate [37], the location factor finally equals $0.75 * 0.137/0.121 = 0.849$.

The inflation factor was determined using the ratio of the Chemical Engineering Plant Cost Index (CEPCI) between the current year (2025) and the base year (2003). Using the most recent CEPCI value for 2025, which is 791.5 [38], and the base year value of 532.9, the inflation factor is calculated as:

$$IF = \frac{791.5}{532.9} = 1.485$$

This factor was applied to adjust all base-year equipment costs to reflect current economic conditions.

Final equipment costs were calculated by multiplying all factors (location, material, and inflation) by the bare costs. Installation costs are equipment costs times installation factors (Table 7.2), depending on the unit.

Table 7.2. Installation factors for equipment.

Equipment Type	Installation factor
Compressor	2.5
Distillation columns	4
Heat exchangers	3.5
Pumps	4

7.2 Capital Investment Estimation

ISBL was calculated by summing up all the installation costs of major equipment. Following the calculation of the ISBL, the OSBL, D&E, and contingency values were estimated

as 30%, 30%, and 10% of the ISBL, respectively. These values were taken from the book, considering that our process involves fluids only [34]. Capital investment estimations are given in Table 7.3.

Table 7.3. Capital investment estimation.

Cost	Amount
ISBL	\$ 47,740,414.11
OSBL	\$ 14,322,124.23
Design & Engineering	\$ 18,618,761.50
Contingency	\$ 6,206,253.83
Total	\$ 86,887,553.68

7.3 Operation Labor Estimation

To calculate the cost of operating labor, the equation by Alkhayat and Gerrard [39] was used:

$$N_{OL} = (6.29 + 31.7 P^2 + 0.23 N_{np})^{0.5} \quad (7.2)$$

where, N_{OL} is the number of operators per shift, P is the processing steps number with particulate solids handling, and N_{np} is the process steps without solids (including compression, towers, heating, cooling, mixing, and reaction). In this case, P is 0.

$$N_{np} = \Sigma \text{Equipment use} \quad (7.3)$$

The calculations for N_{np} are given in Table 7.4.

Table 7.4. The equipment included in the N_{np} calculations.

Equipment type	Number
Reactor	1
Distillation column	3
Compressor	1

Heat exchanger	4
N_{np}	9

The N_{OL} is calculated to be 2.89. If the plant is functional for 24 hours a day for 365 days a year (including downtime), and each day is made of three 8-hour shifts, this results in 1095 shifts a year. A single operator works 48 weeks a year, 5 full working days (8 hours) shifts a week, resulting in 240 shifts a year. Therefore, the number of operators needed to provide all the shifts in a year is 4.563. The total number of plant operators is:

$$4.563 * N_{OL} = 13.19$$

Rounding up to the nearest integer, the number of operators for the plant is 14.

The average salary of an engineer in Kazakhstan is around 6000000 KZT/yr [40], which is equal to 11 484.78 USD/yr. Operating labor cost is therefore:

$$C_{OL} = \text{Number of operators} * \text{Average salary} = 14 * 11\,484.78 = 160\,786.92 \text{ USD/yr}$$

7.4 Fixed Costs of Production

The fixed operating cost includes operating labor, supervision, direct salary overhead, maintenance, property tax and insurance, rent of land, general plant overhead, and allocated environmental charges [34]. The operating labor is estimated in the previous section. Supervision is usually taken as 25% of operating labor [34]. Direct salary overhead is 40 to 60% of operating labor plus supervision. Maintenance is estimated as 3 to 5% of ISBL investment [34]. The property taxes and insurance are typically 1 to 2% of ISBL fixed capital [34]. The rent of land is estimated as 1 to 2% of ISBL plus OSBL investment [34]. General plant overhead is typically taken as 65% of total labor (including supervision and direct overhead) plus maintenance. Allocated environmental charges to cover superfund payments are 1% of the ISBL plus OSBL cost [34]. The fixed operation cost of the plant is summarised in Table 7.5 (all the calculations can be found in ESI).

Table 7.5. Fixed operation cost estimation.

Fixed cost	Amount
Operating labor	\$ 160,786.92
Supervision	\$ 40,196.73
Direct salary overhead	\$ 100,491.83
Maintenance	\$ 1,909,616.56

Property taxes and insurance	\$ 954,808.28
Rent of land	\$ 1,241,250.77
General plant overhead	\$ 1,437,209.83
Allocated environmental charges	\$ 620,625.38
Total Fixed Cost	\$ 6,464,986.30

7.5 Variable Costs of Production

The total price of raw materials, utilities, and consumables (catalyst) adds up to give the variable cost of production, which is given in Table 7.6. Utilities were taken from APEA software.

Table 7.6. Variable cost of production.

Raw materials	Rate, kg/year	Price, \$/kg	Total cost, \$
Methanol	287,750,752.42	0.35 [27]	100,712,763.35
C ₄ mixture	1,181,887,964.33	0.2 [41]	236,377,592.87
Consumables	Rate, kg/year	Price, \$/kg	Total cost, \$
Amberlyst 15	1676.544	2 [42]	3,353.09
Utilities	-	-	59,447,300.00
		Total VC	\$ 396,541,009.30

Prices of methanol and Amberlyst 15 were compared on the Chinese markets, and the most adequate numbers were taken. Regarding C₄'s mixture, it was decided to buy local liquefied petroleum gas, which is relatively cheap (approximately 0.2 \$/kg). However, if we consider a wholesale purchase, the price per kg is going to be reduced to about 0.1 \$/kg, which in turn makes the process more profitable [41]. The mass flow rate of the catalyst per year (tentative) was calculated by dividing the catalyst loading by its lifespan, which is 2 years [43].

7.6 Cash Flow and Profitability Estimation

The working capital is estimated as 7 weeks' cash cost of production minus 2 weeks' feedstock costs plus 1% of the fixed capital investment [34]. Revenue is calculated considering the cost of MTBE which is 0.93\$/kg [44].

The linear depreciation model was applied for 15 years.

Corporate income tax is equal to 20% of the taxable income (EBIT).

The interest rate is assumed to be 12%.

All the detailed calculations are given in the ESI. The graph for the Net Present Value for the first 20 years of plant operation are given in Figure 7.1.

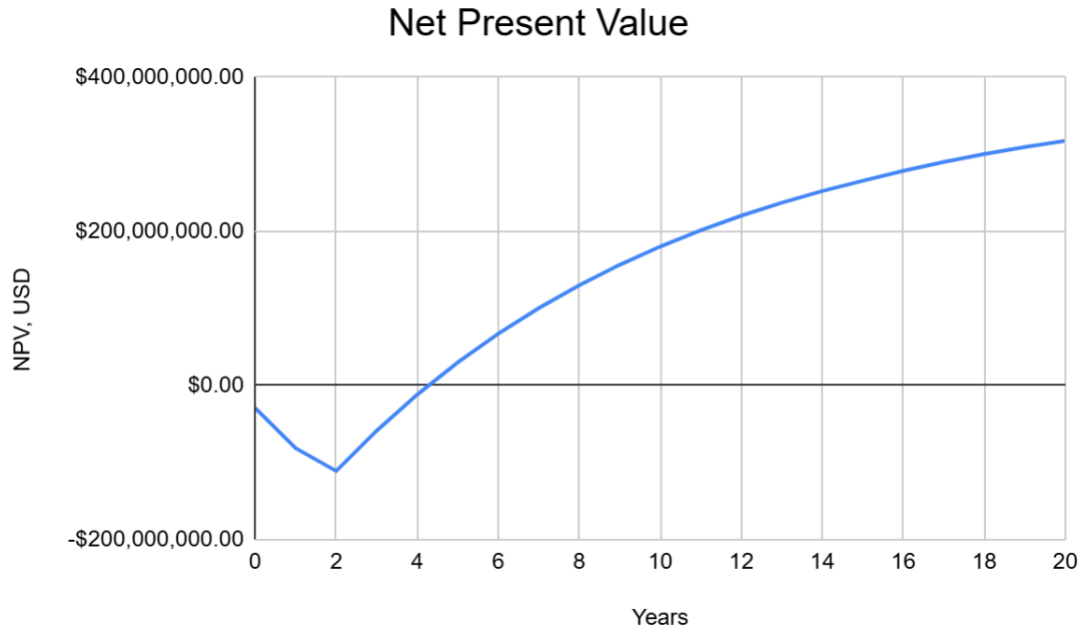


Figure 7.1. The Net Present Value for the first 20 years of operation.

Other assumptions include the fact that total capital investments were divided into 3 years: 30% in the year zero, 60% in the first operation year, and 10% in the third. The plant starts to operate in year 2, and the capacity is 50%, before working at full capacity starting from year 3.

The average cash flow is found to be \$60,979,032.02, and the payback period is 4.28 years. Other economic indicators are summarised in Table 7.7.

Table 7.7. Economic parameters for profitability estimation.

Name	Period	Amount
NPV	10 years	\$180,376,249.30
	20 years	\$317,607,774.01
	30 years	\$363,732,162.85

Return on Investment (ROI)	10 years	20.76%
	20 years	18.28%
	30 years	13.95%
IRR	10 years	39%
	20 years	41%
	30 years	41%

Based on the economic parameters presented above the plant is estimated to be feasible.

Chapter 8. Conclusions and Future Work

In conclusion, a comprehensive report about the design of a plant producing MTBE in Kazakhstan was done. Main parameters like process selection, kinetic modelling, material balance, major and minor equipment design, plant location, environment and economic feasibility were assessed thoroughly.

MTBE of Grade B from “ST RK 2533-2021” was chosen to synthesize from methanol and isobutylene as a main process with production rate 563.5 kt per year. Kinetics of the reaction were validated using Aspen Plus v14 software. There are 4 main units in the plant: 1 reactor and 3 distillation columns. Industrial zone in Kyzylorda was chosen and environmental effects of the waste streams were addressed. Regarding the feasibility of the plant, it was calculated that the payback period will be 4.28 years with average cash flow of \$60,979,032.02.

There are several limitations that were not assessed during the design. It was assumed that mixture of gases would be at 1 bar, but it is usually under high pressure, therefore thorough design of C-101 unit was not really necessary. Instead of designing a C-101 unit, the T-102 unit could be designed properly. Additionally, side products like diisobutene and methyl-sec-butyl-ether were not considered, even though they are usually present at very low amounts. Lastly, due to lack of data on the cost of reagents, economic analysis may not be as accurate as desired.

Reference List

- [1] Cheméo. (n.d.). Cheméo. <https://www.chemeo.com/cid/50-231-9/Propane-2-methoxy-2-methyl>
- [2] Zaretskii, M. I., Rusak, V. V., & Chartov, E. M. (2012). MTBE in extraction processes. *Coke and Chemistry*. <https://doi.org/10.3103/s1068364x12120083>
- [3] *Analysis of Mtbe as an Oxygenate Additive to Gasoline. (2014, March)*. *Journal of Engineering Research and Applications*. <https://dl1wqtxts1xzle7.cloudfront.net/33501855/DS4301712718-libre.pdf>
- [4] Ershov, M., Potanin, D., Tarazanov, S., Abdellatief, T. M. M., & Kapustin, V. (2020). Blending characteristics of Isooctene, MTBE, and TAME as gasoline components. *Energy & Fuels*, 34(3), 2816–2823. <https://doi.org/10.1021/acs.energyfuels.9b03914>
- [5] Kaldygozov, E., Abdikerimov, B., Talapbek, T., & Kapustin, V. (2020). INFLUENCE OF OXYGENATE ADDITIVES ON THE DETONATION AND ENVIRONMENTAL PROPERTIES OF COMMERCIAL AUTOMOBILE GASOLINE COMPONENTS. *Industrial Technology and Engineering*, 2(35), 20-24. <https://ite.auezov.edu.kz/index.php/engineering/article/download/66/59>
- [6] “Standard Specification for Methyl Tertiary-Butyl Ether (MTBE) for Blending With Gasolines for Use as Automotive Spark-Ignition Engine Fuel1,” *compass.astm.org*, Jul. 21, 2021. <https://compass.astm.org/document/?contentCode=ASTM%7CD5983-21%7Cen-US&proxycl=https%3A%2F%2Fsecure.astm.org&fromLogin=true>
- [7] “ЭФИР МЕТИЛ-ТРЕТ-БУТИЛОВЫЙ. Технические условия. СТ РК 2533-2021.” https://shcc.kz/f/st_rk_2533-2021.pdf
- [8] “Казахстан увеличивает производство и экспорт нефтехимии | Petrocouncil,” *Petrocouncil.kz*, Feb. 20, 2024. <https://petrocouncil.kz/kazakhstan-uvelichivaet-proizvodstvo-i-eksport-neftehimii/>
- [9] G.J. Hatchings, C. P. Nicolaidis, and M. S. Scurrrell, “Developments in the production of methyl tert-butyl ether,” *Catalysis Today*, vol. 15, no. 1, pp. 23–49, May 1992, doi: [https://doi.org/10.1016/0920-5861\(92\)80121-3](https://doi.org/10.1016/0920-5861(92)80121-3).
- [10] Fahad, S. (2008). Modeling and simulation of a reactive distillation unit for production of MTBE . *میتل ثالثی بیوتیل اییثر نمذجة ومحااة وحدة تقطير متفاعل لإنتاج مادة MTBE*. <https://citeseerx.ist.psu.edu/document?repid=rep1&type=pdf&doi=7bc6374b6e20d7862d9dcc8c9c21ff1fedf5b33f>
- [11] Singh, Sanjay, Jha, H., Tanushree, Babode, U., & Malviya, L. (2015, December). Modelling and simulation of conventional distillation, reactive distillation column and divided wall distillation column for the production of methyl-tert-butyl-ether (MTBE) using Aspen Plus. https://www.researchgate.net/publication/289532361_MODELLING_AND_SIMULATION_OF_CONVENTIONAL_DISTILLATION_REACTIVE_DISTILLATION_COLUMN_AND_DIVIDED_WALL_DISTILLATION_COLUMN_FOR_THE_PRODUCTION_OF_METHYL-TERT-BUTYL-ETHER_MTBE_USING_ASPEN_PLUS

- [12] Zhang, T., Datta, R., & Department of Chemical and Biochemical Engineering, The University of Iowa, Iowa City, Iowa 52242. (1995). Integral Analysis of Methyl Tert-Butyl Ether Synthesis Kinetics. *Ind. Eng. Chem. Res.*, 730–740.
- [13] Towler, G., & Sinnott, R. (2012). Heat-Transfer equipment. In *Elsevier eBooks* (pp. 1047–1205). <https://doi.org/10.1016/b978-0-08-096659-5.00019-5>
- [14] Max S. Peters, Klaus D. Timmerhaus, and R. Ronald E. West, *Plant Design and Economics for Chemical Engineers*, Fifth Edition. Mc Graw Hill, 2003. Available: <https://caf-corporation.com/caf-capex/wp-content/uploads/2021/07/Plant-Design-and-Economics-for-Chemical-Engineers-PDFDrive.com-.pdf>
- [15] Cortez, R. (2008). ASME SECTION II D-Properties (Customary) Materials. *www.academia.edu*. https://www.academia.edu/45190844/ASME_SECTION_II_D
- [16] Coker, A. K. (2015). Compression Equipment (Including Fans). Ludwig’s Applied Process Design for Chemical and Petrochemical Plants, 729–978. [Sci-Hub | Compression Equipment \(Including Fans\). Ludwig’s Applied Process Design for Chemical and Petrochemical Plants, 729–978 | 10.1016/B978-0-08-094242-1.00018-8](https://doi.org/10.1016/B978-0-08-094242-1.00018-8)
- [17] Brown, R. N. (2005). *Compressors: Selection and Sizing*. Gulf Professional Publishing.
- [18] Lüdtke, K. H. (2004). *Process centrifugal compressors: Basics, Function, Operation, Design, Application*. Springer Science & Business Media.
- [19] 17-4PH Stainless Steel. (2025) *Gnee Stainless Steel*. <https://gneestainlesssteel.com/17-4ph-stainless-steel/>
- [20] Bahadori, A. (2014). *Corrosion and materials selection: A Guide for the Chemical and Petroleum Industries*. John Wiley & Sons. Section 3.2.29.
- [21] R. Kane, J. Maldonado, and L. Klein, “Stress Corrosion Cracking in Fuel Ethanol: A Newly Recognized Phenomenon,” Jan. 01, 2004. https://www.researchgate.net/publication/254545755_Stress_Corrosion_Cracking_in_Fuel_Ethanol_A_Newly_Recognized_Phomenon
- [22] “316L Stainless Steel Chemical Compatibility Chart Industrial Specialties Mfg. and IS MED Specialties,” 2020. Available: <https://marketing.industrialspec.com/acton/attachment/30397/f-003a/1/-/-/-/316l-stainless-steel-chemical-compatibility-from-ism.pdf>
- [23] Gavin Towler. (2012, January 13). *Heat-transfer equipment*. Chemical Engineering Design (Second Edition). <https://www.sciencedirect.com/science/article/pii/B9780080966595000195>
- [24] Coker, A. K. (2015). Distillation, packed towers, petroleum fractionation, gas processing and dehydration. Ludwig’s Applied Process Design for Chemical and Petrochemical Plants, 679-686. <https://doi.org/10.1016/C2009-0-27075-9>
- [25] André B., Burak E., Boelo S., (2020). *Industrial Separation Processes: Fundamentals*. [Knovel - Industrial Separation Processes - Fundamentals](https://www.knovel.com/industrial-separation-processes-fundamentals)
- [26] R. Turton, R. C. Bailie, W. B. Whiting, J. A. Shaeiwitz, and D. Bhattacharyya, “Analysis, Synthesis, and Design of Chemical Processes Fourth Edition,” Pearson Education, Inc,

2012. Available:
https://moodle.nu.edu.kz/pluginfile.php/1007924/mod_resource/content/0/1.1%20-%20Heuristics%20from%20Turton%20course%20book.pdf
- [27] “High Purity 99.9% Methanol / Methyl Alcohol CAS 67-56-1 for Best Price,” *Made-in-China.com*, 2025. <https://nearchem.en.made-in-china.com/product/YZCaiWRTHurv/China-High-Purity-99-9-Methanol-Methyl-Alcohol-CAS-67-56-1-for-Best-Price.html>
- [28] “Information about the city,” *Invest.gov.kz*, 2024. <https://kyzylorda.invest.gov.kz/about/info/>
- [29] “SEZ or IZ: Which site to choose?,” *Invest.gov.kz*, 2024. <https://invest.gov.kz/doing-business-here/fez-and/sez-or-iz-which-site-to-choose/>
- [30] J. Ott *et al.*, “Methanol,” *Ullmann’s Encyclopedia of Industrial Chemistry*, 2012, doi: https://doi.org/10.1002/14356007.a16_465.pub3.
- [31] Kaviraj, A., Bhunia, F., & Saha, N. C. (2004). Toxicity of Methanol to Fish, Crustacean, Oligochaete Worm, and Aquatic Ecosystem. *International Journal of Toxicology*, 23(1), 55–63. doi:10.1080/10915810490265469
- [32] Al-Dawery, S. K., & Aljundi, I. H. (2015). Methanol removal from methanol-water mixture using activated sludge, air stripping and adsorption process: Comparative study. *Journal of Engineering Science and Technology*, 10(12), 1615-1627.
- [33] “Об утверждении критериев оценки экологической обстановки территорий - ИПС ‘Әділет,’” *Adilet.zan.kz*, 2021. <https://adilet.zan.kz/rus/docs/V2100023994>.
- [34] Towler, G., & Sinnott, R. (2012). Capital cost estimating. In *Elsevier eBooks* (pp. 307–354) <https://doi.org/10.1016/b978-0-08-096659-5.00007-9>
- [35] “GBIChina | China Industry map,” *Gbichina.com*, 2018. <https://www.gbichina.com/page/china-industry-map/>
- [36] MACROTRENDS. (2025, April 18). *Dollar Yuan Exchange Rate - 35 year historical chart*. <https://www.macrotrends.net/2575/us-dollar-yuan-exchange-rate-historical-chart>
- [37] *Chinese yuan rmb to US dollars Exchange Rate History | Currency Converter | Wise*. (n.d.). <https://wise.com/gb/currency-converter/cny-to-usd-rate/history>
- [38] *Redirect notice*. (n.d.). <https://www.google.com/url?q=https://www.chemengonline.com/plant-cost-index-beta/&sa=D&source=editors&ust=1745000813586318&usg=AOvVaw10bQn3HUY0y-vFZ0tytxUx>
- [39] R. Turton, R. C. Bailie, W. B. Whiting, J. A. Shaeiwitz, and D. Bhattacharyya, *Analysis, Synthesis, and Design of Chemical Processes* Fourth Edition, 4th ed. Prentice Hall, 2012
- [40] Борисевич, М. (2024, October 16). *Высокооплачиваемые профессии в Казахстане, которые актуальны в 2023 году*. NUR.KZ. <https://www.nur.kz/family/self-realization/1665557-samyevysokooplachivaemyeprofessii/?ysclid=m9jre12qrd472704072>

- [41] BES.media. (2025, January 17). Цены на сжиженный газ вырастут в Казахстане с 1 февраля. *BES.media*. <https://bes.media/news/tseni-na-szhizhenniy-gaz-virastut-v-kazahstane-s-1-fevralya-d20f03/>
- [42] *Polymeric catalyst resin for MTBE and TaMe equal to amberlyst 15 wet.* (n.d.). Made-in-China.com. https://sunresin.en.made-in-china.com/product/FdetahoVkbpK/China-Polymeric-Catalyst-Resin-for-Mtbe-and-Tame-Equal-to-Amberlyst-15-Wet.html?pv_id=1ip2ef71aba1&faw_id=1ip2egl3ja93
- [43] DuPont. (n.d.). *Good as gold.* <https://www.dupont.com/content/dam/water/amer/us/en/water/public/documents/en/IER-AmberLyst-Good-as-Gold-Br-45-D03627-en.pdf>
- [44] I. Group, “Methyl Tert-Butyl Ether (MTBE) Price Trend, News, Monitor, Forecast & Analysis,” *Imarcgroup.com*, 2023. <https://www.imarcgroup.com/methyl-tert-butyl-ether-pricing-report>
- [45] *Cheméo.* (n.d.). Cheméo. <https://www.cheméo.com/cid/50-231-9/Propane-2-methoxy-2-methyl>
- [46] *PubChem.* (n.d.-c). *Methyl Tert Butyl Ether.* PubChem. <https://pubchem.ncbi.nlm.nih.gov/compound/15413>
- [47] Hao Lianping. MTBE Market to Be Governed by Demand. *China Chemical Reporter*. 2017;28(6):19-34. Accessed September 26, 2024. <https://research.ebsco.com/linkprocessor/plink?id=b67efa78-9ffc-30e2-afb1-846ada0b9bb5>
- [48] Mi Duo, Zu Siya. MTBE Consumption not Optimistic Under the Impact of New Energy Vehicles. *China Chemical Reporter*. 2022;33(10):23-26. Accessed September 26, 2024. <https://research.ebsco.com/linkprocessor/plink?id=79087c1d-22e2-3f99-a8af-2ac277084073>
- [49] The World Bank, “World Development Indicators | DataBank,” *Worldbank.org*, 2024. <https://databank.worldbank.org/reports.aspx?source=world-development-indicators>

Appendix

Appendix A. Properties of MTBE

Table A.1. Main properties of MTBE [45].

CAS name	Methyl tert-butyl ether
IUPAC Name	MTBE
CAS registry number	1634-04-4
Chemical formula	$(\text{CH}_3)_3\text{COCH}_3$
Molecular weight	88.15

Table A.2. Main physical properties of MTBE.

Density (g/cm^3 , 20°C)	0.740 [46]
Conductivity ($\text{W}/\text{m}\cdot\text{K}$, 25°C)	0.2 [45]
Water solubility (mol/l)	0.57544 [46]
Refractive index	1.369 (20°C) [46]
Freezing point	-108.59±0.07 °C [46]
Boiling point	55.1 °C [46]
Vapor pressure (kPa, 25°C)	33.39 [46]

Appendix B. Physical and thermodynamic data.

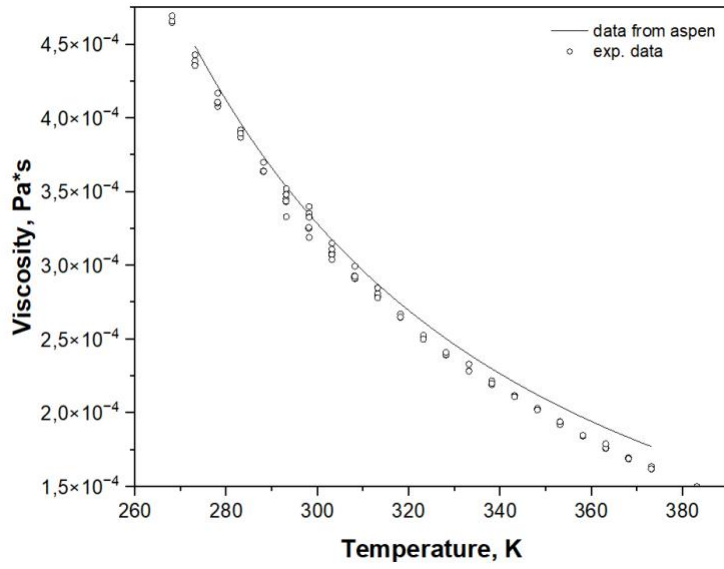


Figure B.1. Viscosity of MTBE vs temperature. (NIST)

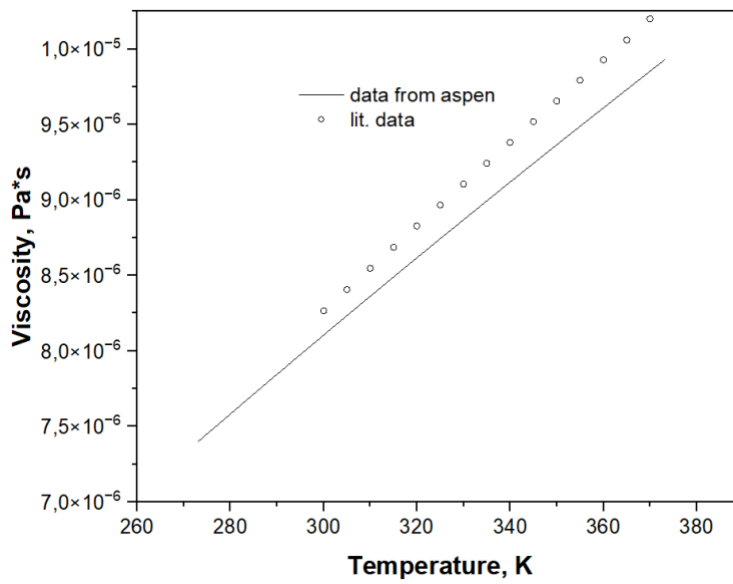


Figure B.2. Viscosity of isobutylene vs temperature.

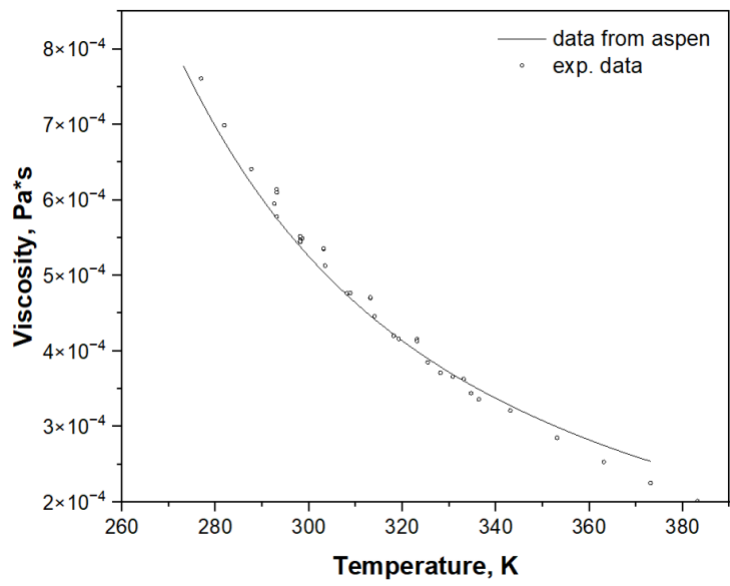


Figure B.3. Viscosity of methanol vs temperature.

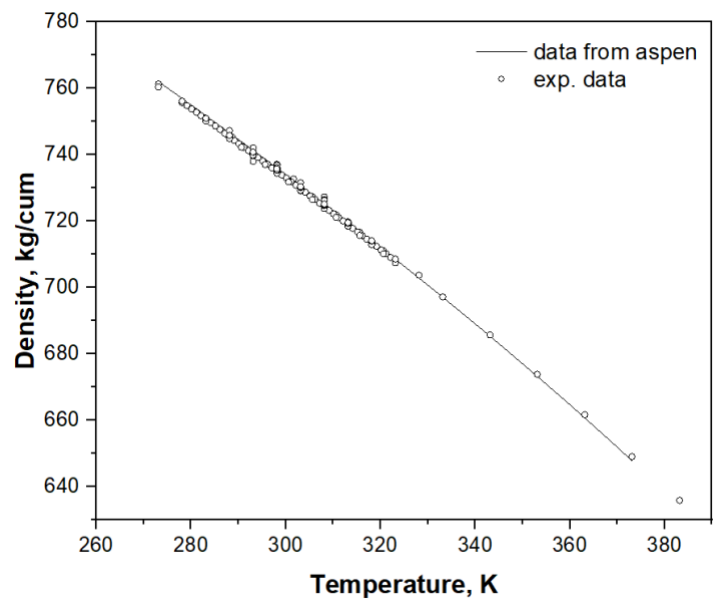


Figure B.4. Density of MTBE vs temperature.

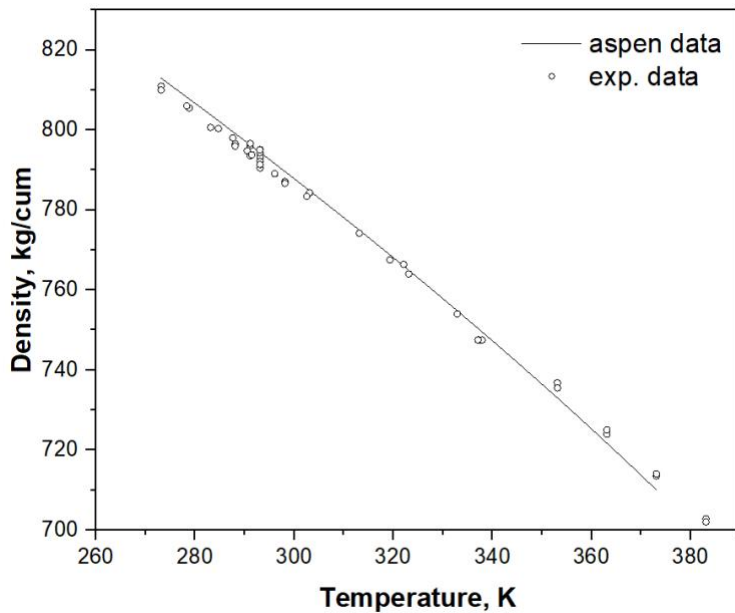


Figure B.5. Density of methanol vs temperature.

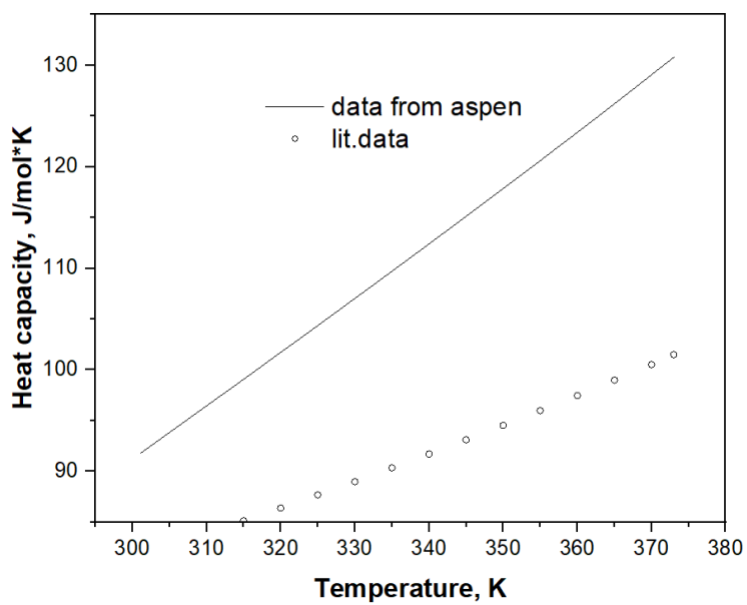


Figure B.6. Heat capacity of methanol vs temperature.

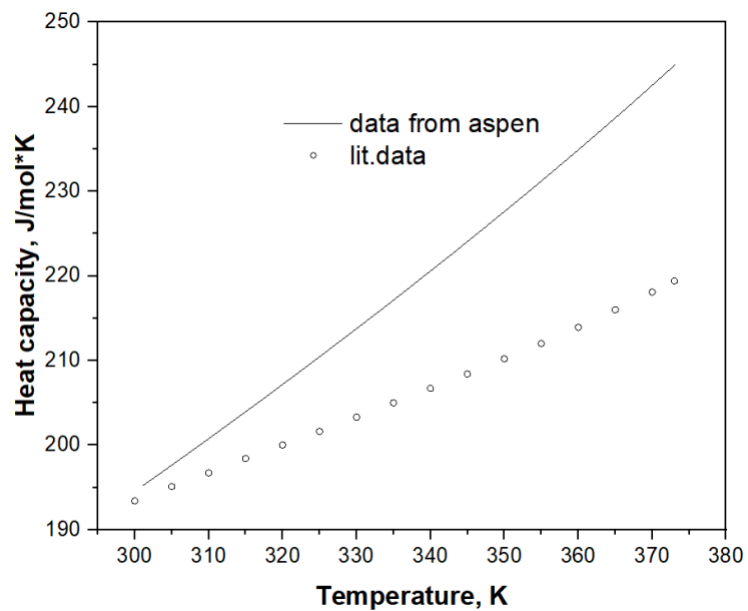


Figure B.7. Heat capacity of MTBE vs temperature.

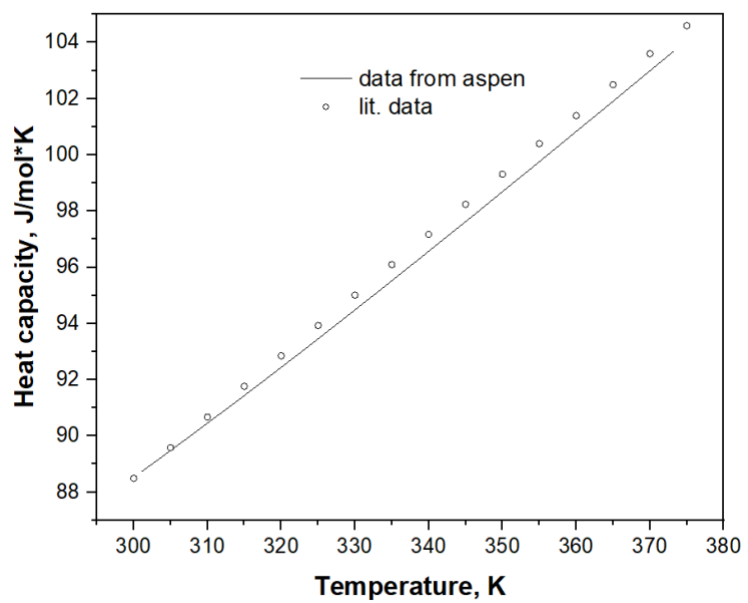


Figure B.8. Heat capacity of gas phase isobutylene vs temperature.

Appendix C. Binary mixtures

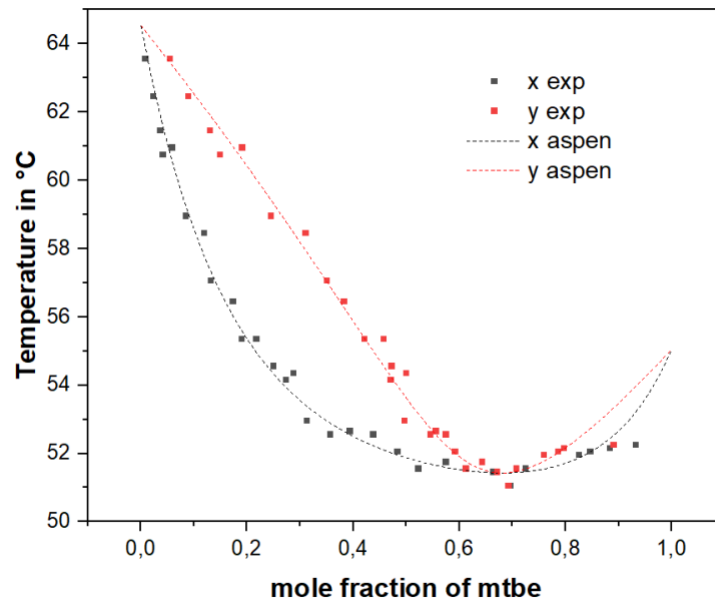


Figure C.1. T-xy diagram of MTBE and methanol.

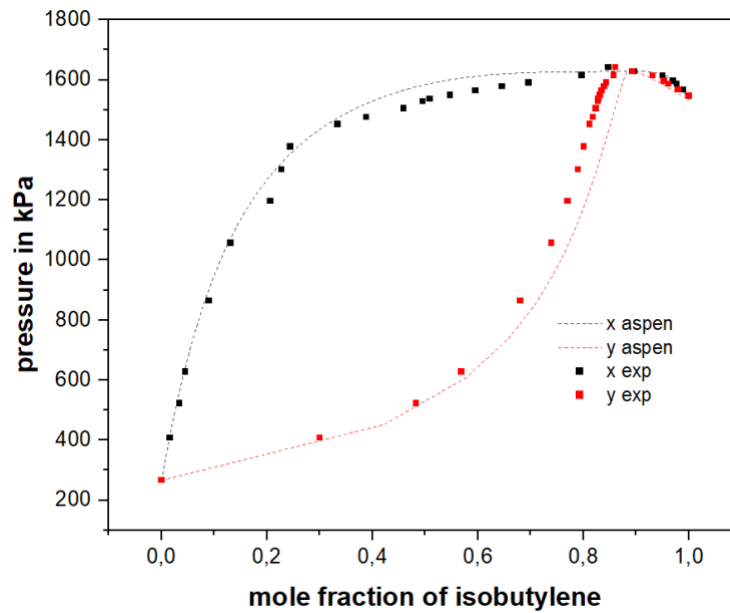


Figure C.2. P-xy diagram of methanol and isobutylene.

Appendix D. Market analysis

Table D.1. MTBE production and demand in China, 2007-2021 [47, 48]

Year	Production Capacity, 10kt/year	Demand, 10kt/year
2007	234.90	230.00
2008	302.30	292.00
2009	293.50	328.00
2010	384.38	451.80
2011	416.60	468.89
2012	425.60	438.44
2013	498.90	529.70
2014	607.10	635.87
2015	715.28	733.29
2016	Not available	Not available
2017	1,165.52	1,180.27
2018	1,208.44	1,216.22
2019	1,316.23	1,331.64
2020	1,206.42	1,219.30
2021	1,303.67	1,385.76

Table D.2. Nominal GDP values of China, CIS and Kazakhstan [49].

Year	GDP nominal, billion USD		
	China	CIS	Kazakhstan
2012	8532	2861.912	208
2013	9570	3018.546	236.6

2014	10480	2732.496	221.4
2015	11060	1904.76	184.4
2016	11230	1757.778	137.3
2017	12310	2094.434	166.8
2018	13890	2212.325	179.3
2019	14280	2300.336	181.7
2020	14690	2073.033	171.1
2021	17820	2539.385	197.1
2022	17960	3025.227	225.5

Table D.3. Calculated MTBE demand for CIS and Kazakhstan (based on Chinese data, Excel calculations).

Year	Demand, 10kt/year	
	CIS	Kazakhstan
2012	147.07	36.77
2013	167.08	41.77
2014	165.79	41.45
2015	126.29	31.57
2017	200.81	50.20
2018	193.71	48.43
2019	214.51	46.98
2020	172.06	43.02
2021	197.47	49.37

Appendix E. Reactor R-101.

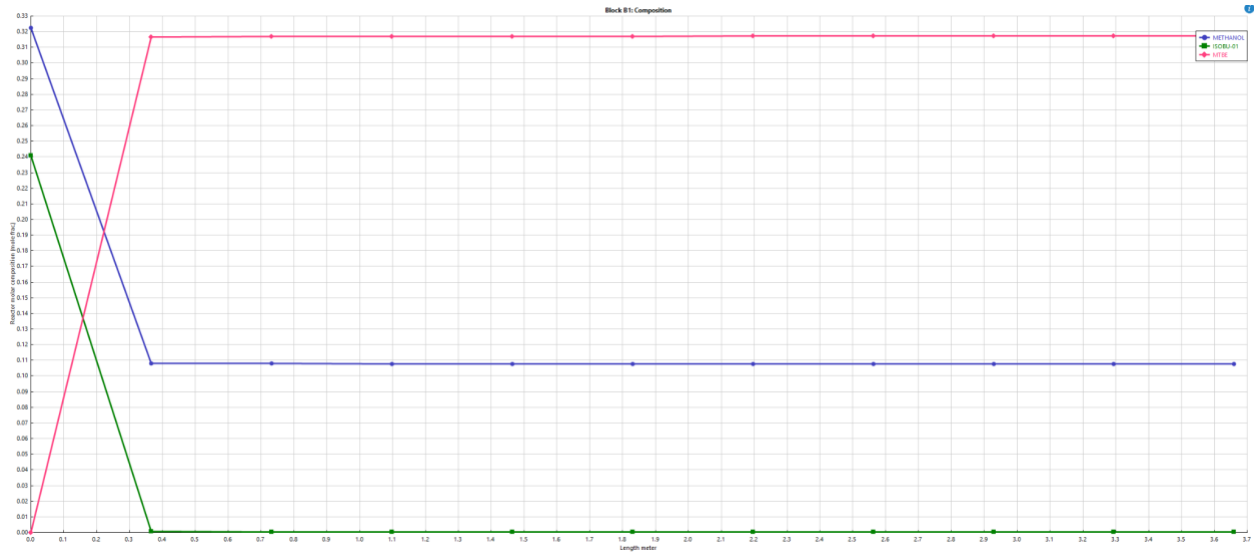


Figure E.1. Molar composition of reactor with cooling water.

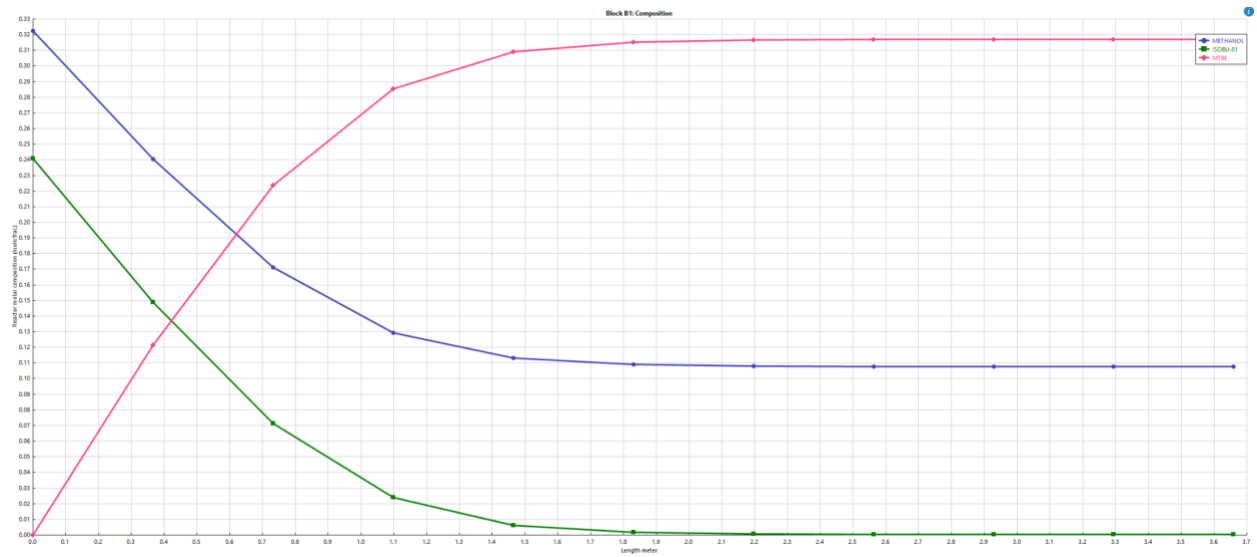


Figure E.2. Molar composition of a constant temperature reactor.

Appendix F. Heat exchanger E-101.

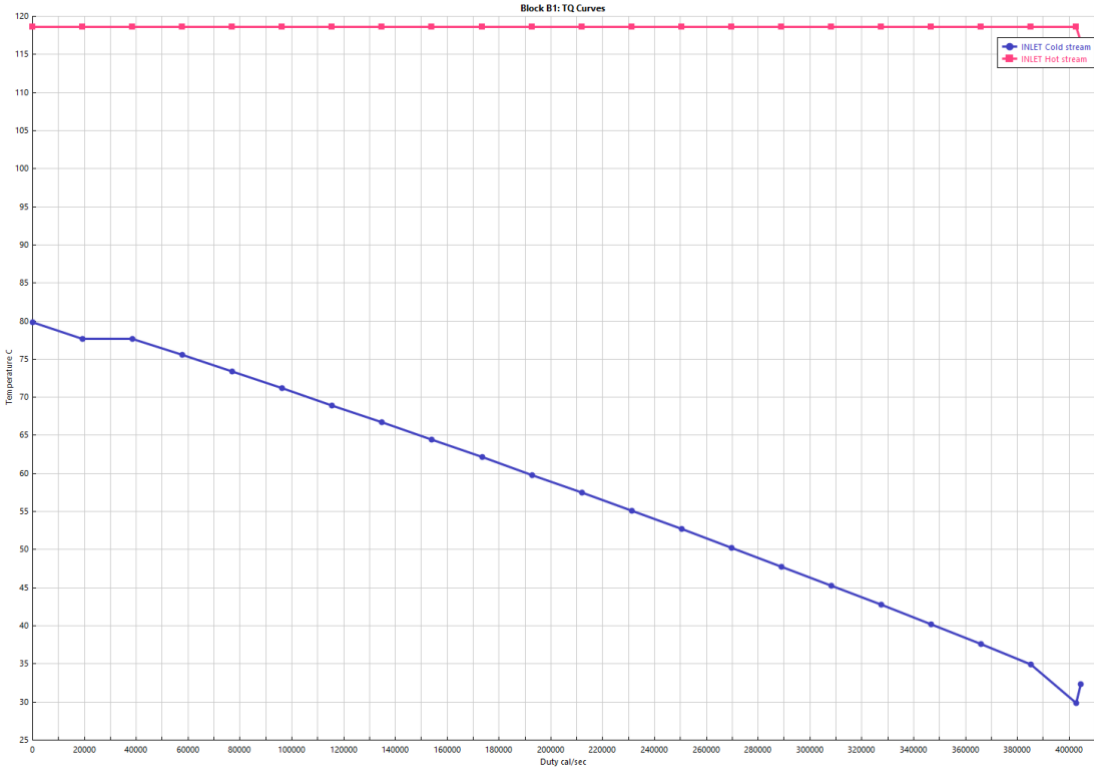


Figure F.1. TQ curve.

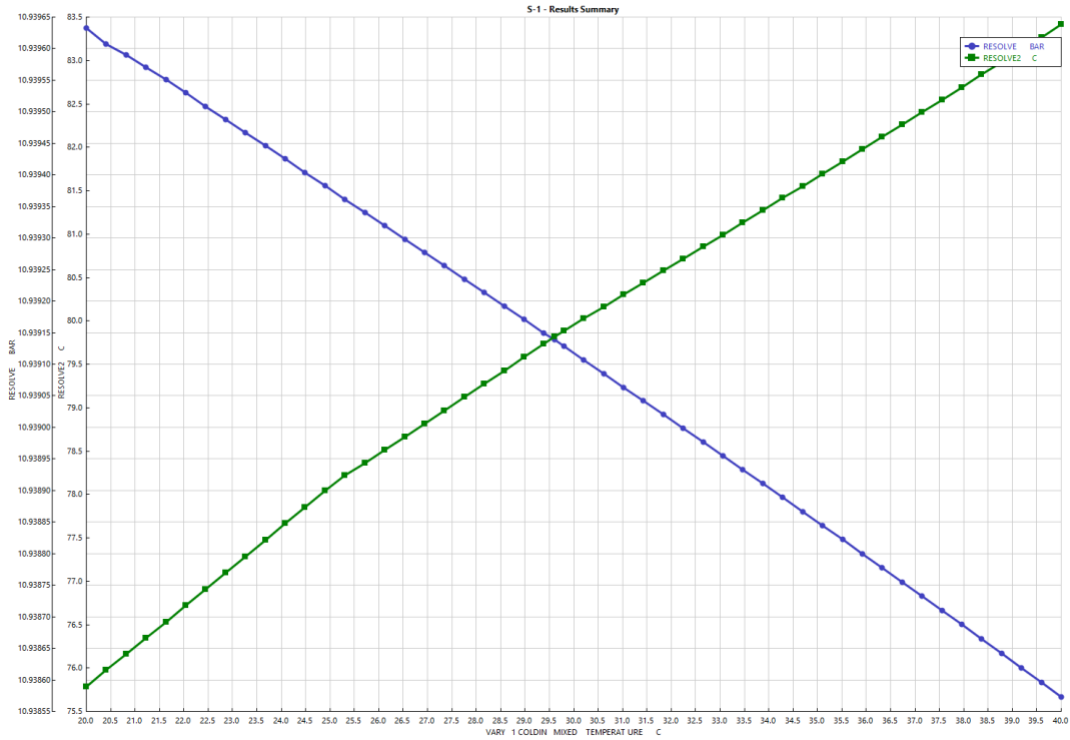


Figure F.2. Sensitivity analysis on changing inlet methanol stream temperature on outlet methanol stream pressure and temperature.

Appendix G. Heat Exchanger E-102.

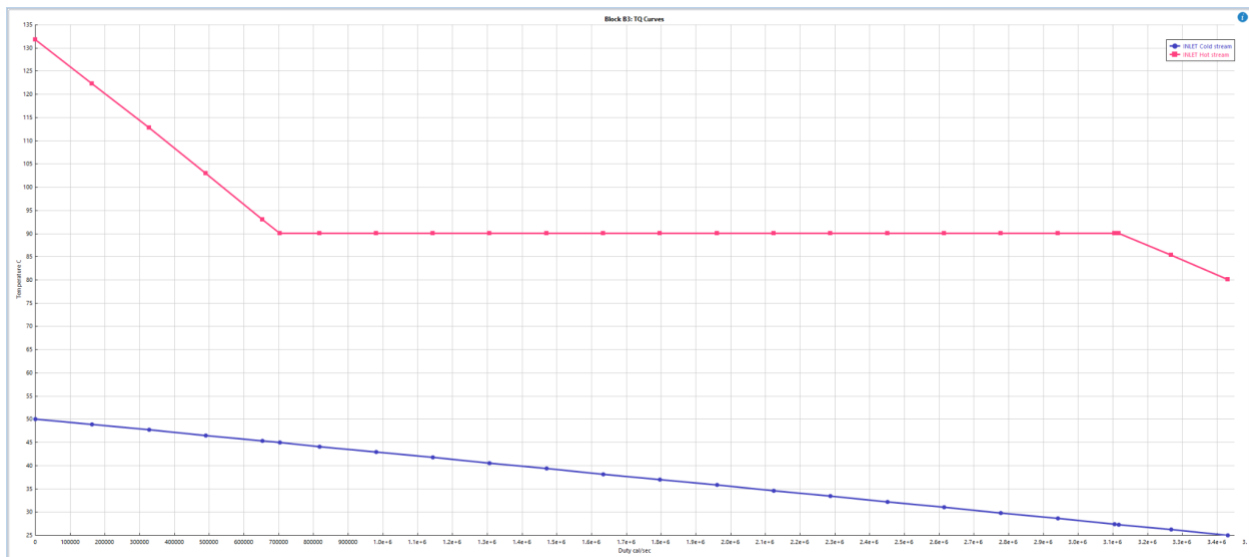


Figure G.1. TQ curve.

Appendix H. Distillation Column T-101.

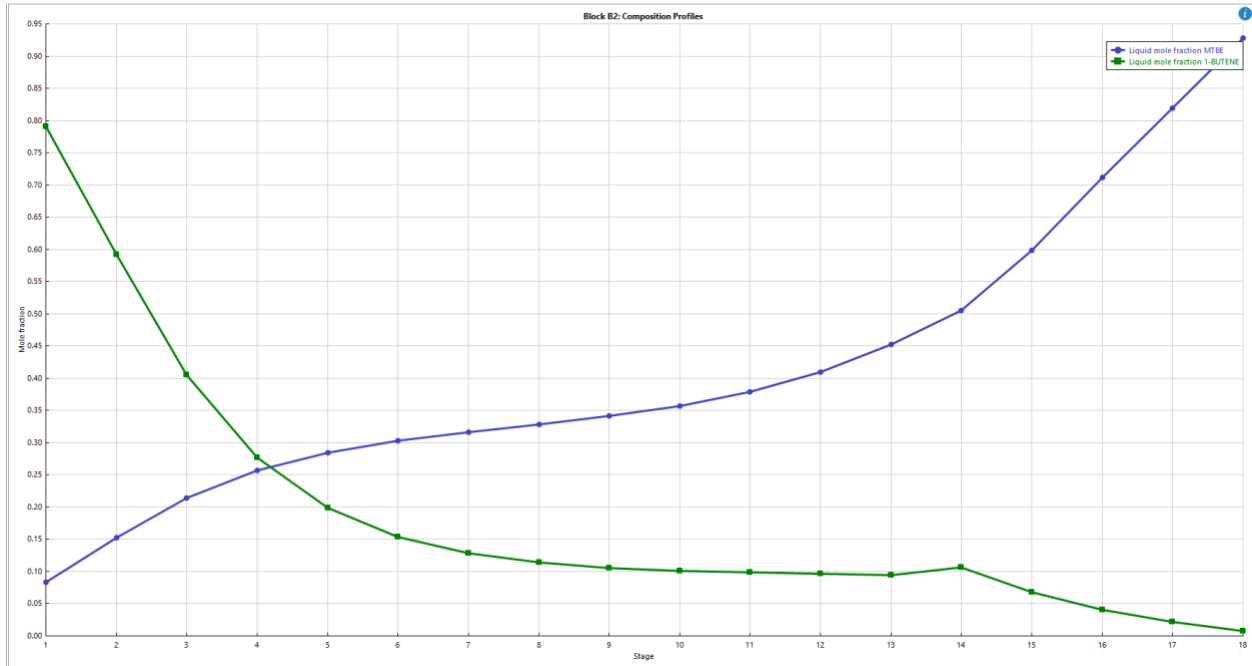


Figure H.1. Composition profile.

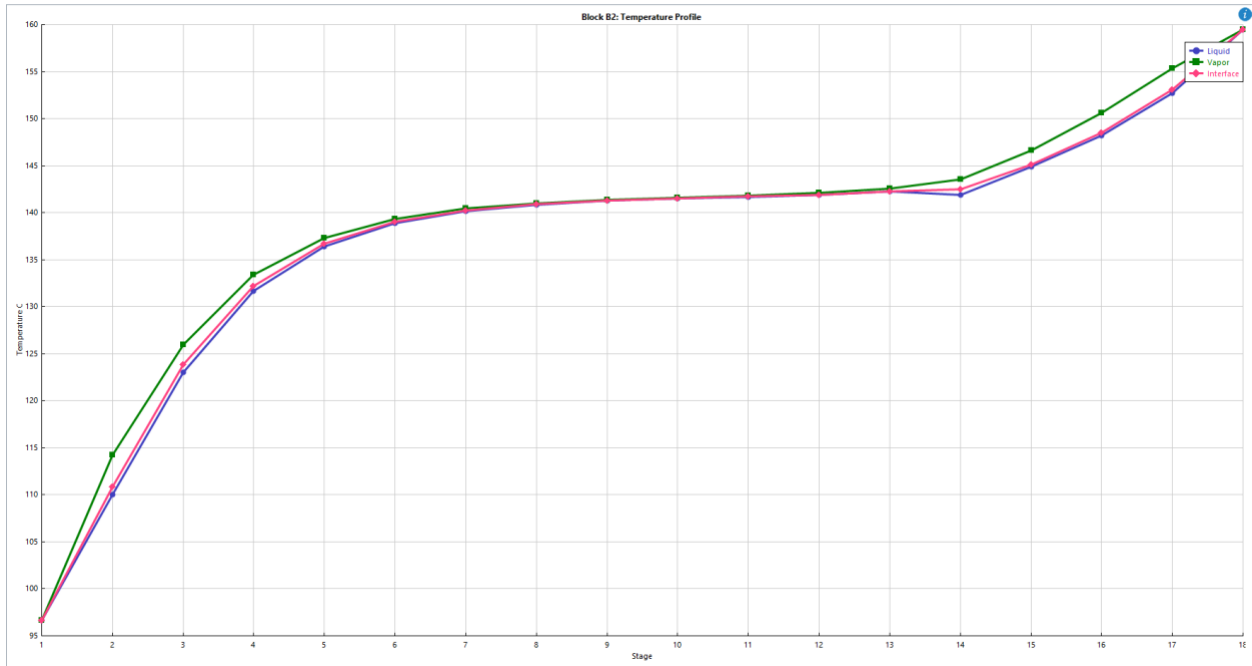


Figure H.2. Temperature profile.

Appendix I. Distillation Column T-103.

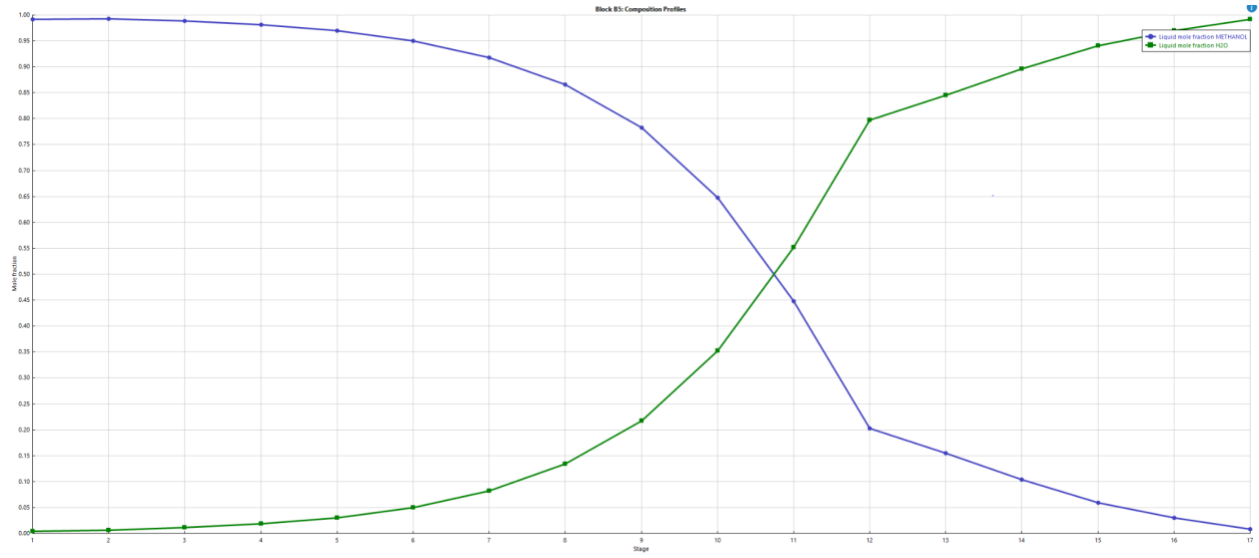


Figure I.1. Composition profile.

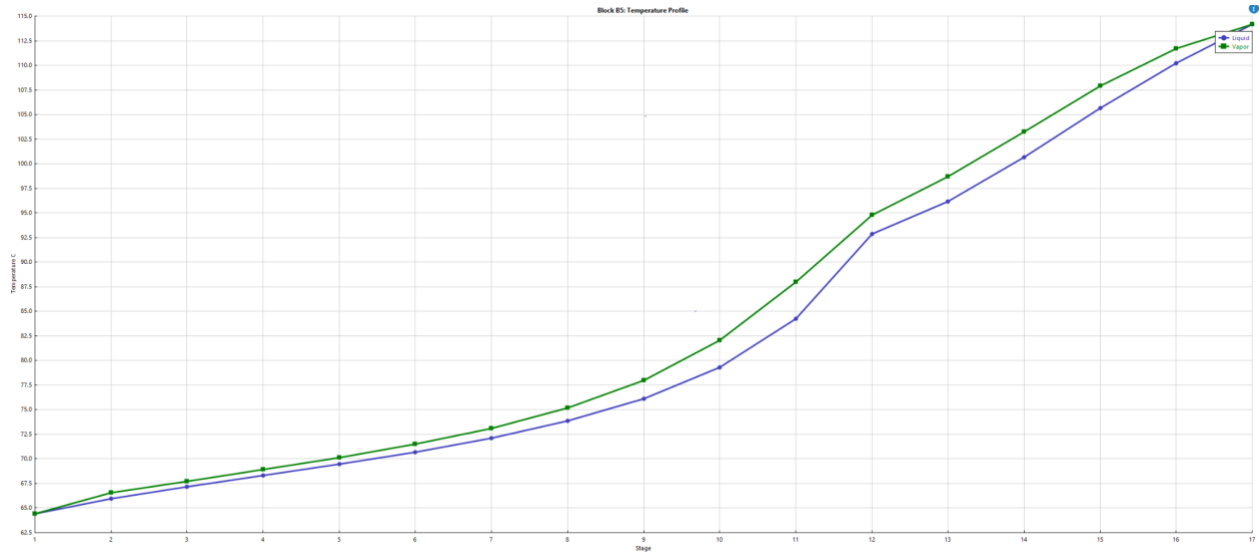


Figure I.2. Temperature profile.